Christie, D.M., Pedersen, R.B., Miller, D.J., et al., 2001
Proceedings of the Ocean Drilling Program, Initial Reports Volume 187

12. Site 1161[1]

Shipboard Scientific Party[2]

PRINCIPAL RESULTS

Site 1161 is located in western Zone A, ~78 km east of the ~127°E fracture zone and 43 km south of Site 1158. The seafloor magnetic age is ~19 Ma. The site was located during the Leg 187 survey transit between Sites 1158 and 1159. The site is in a small, sediment-filled basin in rugged terrain that we interpret as the transferred lithosphere zone of an extinct westward-directed propagating rift system, identified from aeromagnetic data by Vogt et al. (1984). Site 1162 is ~45 km farther south, in a valley formed by this propagating rift. This site is part of the north-south transect in western Zone A; it was intended to check for Indian-type mantle between the previously identified Pacific-type Sites 1158 and 1159. Together with Site 1162, Site 1161 could, if it is of Indian type, test whether rift propagation reintroduced Pacific-type mantle beneath the region.

Hole 1161A was spudded in ~5020 m water depth and was washed through ~116 m of sediment, recovering a single wash barrel containing a slurry of drilling-induced clay pellets with pieces of basalt in the bottom of the core catcher. Rotary drilling continued 29.3 m into volcanic basement, recovering 4.4 m (~15%) of basaltic rubble with fragments of aphyric to plagioclase-olivine phyric basaltic breccia. Between the large clasts is a finer grained breccia with clasts of altered basalt and palagonitized glass in a clay-rich sediment matrix. Hole 1161A was abandoned because of drilling problems.

Hole 1161B was spudded 200 m north of Hole 1161B and was washed through ~158 m of sediment with no recovery. Rotary drilling continued only 8.5 m into volcanic basement, recovering 0.9 m (~10%) of aphyric to highly plagioclase-olivine phyric basalt and basaltic breccia similar to that recovered from Hole 1161A. Basalts from both holes are moderately to strongly altered with Fe oxyhydroxide and clay replacing olivine phenocrysts and basaltic groundmass.

[1]Examples of how to reference the whole or part of this volume.
[2]Shipboard Scientific Party addresses.

Ms 187IR-112

A basalt glass from Hole 1161B was analyzed for major and trace elements by shipboard inductively coupled plasma–atomic emission spectrometry (ICP-AES), and a whole rock from Hole 1161A was analyzed by X-ray fluorescence (XRF). The Ba and Zr contents of the glass clearly indicate that it is derived from Indian-type mantle. This occurrence, separated by <1 Ma from the Pacific-type mantle beneath Site 1158, documents a second incursion of Indian mantle into Zone A (Site 1157 documents the first).

OPERATIONS

Transit to Site 1161

The 257-nmi transit between Sites 1160 and 1161 required 33 hr at an average speed of 8 kt. We made the transit at reduced speed so the active heave compensator hydraulic service loop could be repaired. Site 1161 is the northernmost of three potential sites located during our transit survey between Sites 1158 and 1159 (see **"Site Geophysics,"** p. 4, in the "Site 1159" chapter). At 1430 hr on 25 December, we slowed to 6 kt and conducted a south-to-north 3.5-kHz survey over Global Position System (GPS) coordinates of this site. At 1530 hr we dropped a positioning beacon about 1 km north of our original GPS coordinates. This position is closer to the middle of the target sediment pond.

Hole 1161A

After the hydrophones and thrusters were extended and the vessel settled on location, the precision depth recorder (PDR) referenced to the dual-elevator stool indicated a water depth of 5031.4 m below the rig floor. The nine-collar bottom-hole assembly employed at the previous sites was reassembled with a new C-7 four-cone rotary bit and a mechanical bit release. We initiated Hole 1161A at 2330 hr on 25 December and drilled to 116.0 meters below the seafloor (mbsf) before contacting basement. We deepened Hole 1161A by rotary coring from 116.0 to 145.3 mbsf (Cores 187-1161A-2R to 5R) before the hole had to be abandoned because of erratic high torque, rapid penetration, and poor recovery (15%; Table **T1**). A tracer of fluorescent microspheres was deployed on Core 187-1161A-2R. The drill string cleared the seafloor at 1315 hr on 26 December, and we offset in dynamic positioning mode 200 m north.

T1. Coring summary, Site 1161, p. 44.

Hole 1161B

At Hole 1161B, we washed through 158.5 m of sediment before contacting basement and retrieving a wash barrel, which recovered a few pieces of basalt. We advanced Hole 1161B by rotary coring from 158.5 to 167.0 mbsf (Cores 187-1161B-2R and 3R, 10% recovery) with the same poor drilling conditions we experienced in the first hole. Rather than attempting to start a third hole at this site, we decided that we had recovered sufficient material at this site to meet our primary shipboard objectives and to move to our next site. We deployed a second tracer of fluorescent microspheres on Core 187-1161B-2R. The drill bit cleared the seafloor at 0045 hr and the rotary table at 0915 hr on 27 December.

IGNEOUS PETROLOGY

Introduction

Holes 1161A and 1161B were cored into igneous basement from 116.0 to 145.3 and 158.5 to 167.0 mbsf, respectively. Hole 1161A (Sections 1W-CC through 5R-1) was drilled 29.3 m into basement, resulting in 4.39 m of recovered core (15.0% recovery). All recovered material from this hole has been assigned to one lithologic unit: basaltic rubble with intervals of basaltic breccia. The unit is composed of intermingled lithic clasts, derived from aphyric to moderately plagioclase-olivine phyric basalt.

Hole 1161B (Sections 187-1161B-1W-1 through 3R-1) was drilled 8.5 m into basement, resulting in 0.86 m of recovered core (10.12% recovery). This hole also yielded basaltic rubble with intervals of basaltic breccia, similar to the material recovered from Hole 1161A, and all of this material was assigned to a single unit. The material from both holes is interpreted as talus; no primary magmatic stratigraphic significance can be associated with the position of individual pieces in either hole.

Hole 1161A

Unit 1

Unit 1 of Hole 1161A consists of basaltic rubble with several intervals of basaltic breccia (i.e., Sections 3R-2 [Pieces 7, 8, and 11], 4R-1 [Pieces 9–12], and 5R-1 [Pieces 11–14, 17]). At least three different igneous lithologies occur among the rubble clasts (Table T2): (1) light gray, microcrystalline, sparsely to moderately plagioclase-olivine phyric basalt (Fig. F1); (2) medium gray, microcrystalline, aphyric to sparsely plagioclase (± olivine) phyric basalt (Fig. F2); and (3) mottled buff to gray-brown, fine-grained aphyric basalt (Fig. F3). Only the first two lithologies are observed within the breccias. All three lithologies are intermixed throughout the hole, but Type 1 predominates, constituting 61% of the recovered rubble clasts. Type 2 and Type 3 basalts occur in similar proportions (i.e., 17% and 22%, respectively). All basalt types are moderately to highly altered throughout the unit. In highly altered pieces, alteration is characterized by pervasive replacement of olivine phenocrysts and groundmass phases by a mixture of Fe oxyhydroxides and clay; in moderately altered pieces, a similar type of oxidative alteration is concentrated in halos that have formed adjacent to veins, fractures, and outer weathered surfaces (see "Alteration," p. 8).

Petrography of Basaltic Rubble Clasts

Sparsely to Moderately Plagioclase-Olivine Phyric Basalt (Type 1). Type 1 basalt consists of 1%–2% equant olivine and 1%–3% tabular to prismatic plagioclase phenocrysts. Between 20% and 70% of the phenocrysts occur as glomerocrysts. These generally consist of a relatively loose collection of prismatic plagioclase (<3 mm in length) ± small (<1 mm) and equant to skeletal olivine; more rarely these consist of clusters of olivine phenocrysts or microphenocrysts. They probably form by aggregation and/or equilibrium growth of phenocrysts during crystallization of the magma. In contrast, larger plagioclase phenocrysts (3–4 mm) tend to have equant (subhedral) or rounded (anhedral) shapes and occur as solitary crystals. These typically display discontinuous zoning and are sieve-textured, suggesting disequilibrium with the host magma.

T2. Basalt clast types, p. 45.

F1. Moderately plagioclase-olivine phyric basalt (Type 1), p. 13.

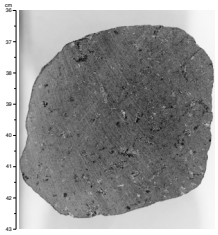

F2. Aphyric to sparsely plagioclase ± olivine phyric basalt (Type 2), p. 14.

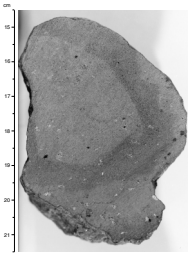

F3. Fine-grained aphyric basalt (Type 3), p. 15.

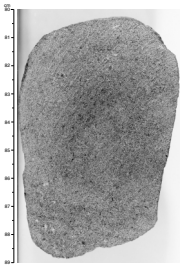

Some smaller prismatic phenocrysts also show sieve textures, but these crystals tend to have fewer embayments, the embayments tend to parallel cleavage or twin planes, and the crystals are less likely to show discontinuous zoning. This suggests that the sieve textures in these crystals developed as a growth feature rather than by partial resorption. All plagioclase phenocrysts show albite twinning and are generally unaltered. Equant olivine phenocrysts (0.5–3 mm) are present throughout and range from subhedral to euhedral. However, fresh olivine is rarely observed, being totally replaced by Fe oxyhydroxides ± clay in most pieces (see **"Alteration,"** p. 8). Two subhedral spinel microphenocrysts containing melt inclusions up to 40 µm were observed in Sample 2R-1, 10–13 cm (Fig. **F4**).

Groundmass textures are microcrystalline to cryptocrystalline, ranging from intersertal (Fig. **F5**) to immature sheaf quench morphologies to spherulitic with decreasing distance from the chilled margins. Acicular to skeletal plagioclase (aspect ratios up to 30:1) forms 20%–40% of the groundmass, and small (<100 µm) equant olivines form 2%–3% of the groundmass. In most cases clinopyroxene is restricted to plumose quench crystal morphologies, but the size of clinopyroxene and Fe-Ti oxide crystals is enhanced adjacent to and within miarolitic cavities (Fig. **F5**), similar to some basalts from Site 1157. In these cavities clinopyroxene forms anhedral, granular to elongate crystals up to 200 µm, and equant Fe-Ti oxides as large as 50 µm are observed. Elsewhere, Fe-Ti oxides occur as minute (<2 µm) equant crystals and make up ~1%–2% of the groundmass. Dark brown mesostasis—which here includes glass plus indistinguishable quench crystals of plagioclase, clinopyroxene, and olivine—makes up >50% of the rock. Vesicles are rare. Where present, they tend to be small (<0.3 mm in diameter), spherical, and lined or filled with clay minerals (see **"Alteration,"** p. 8).

Aphyric to Sparsely Plagioclase (± Olivine) Phyric Basalt (Type 2). Type 2 basalts are similar to those of Type 1 but are distinguished by containing fewer plagioclase phenocrysts (1%–2% tabular to prismatic crystals) and rare olivine microphenocrysts (≤1%). Plagioclase phenocrysts also have a tendency to be small (<1–2 mm long), although large solitary crystals up to 7 mm are also present. The latter tend to be similar to the large plagioclase phenocrysts observed in Type 1 basalts, i.e., they have equant (subhedral) or rounded (anhedral) shapes, display discontinuous zoning, and are sieve textured. Approximately 25% of the phenocrysts occur as glomerocrysts, which in this basalt type are dominated by small prismatic plagioclase crystals. All plagioclase phenocrysts show albite twinning and are generally unaltered. Although not abundant (≤1%), equant olivine microphenocrysts (<1 mm) are usually present and range from subhedral to euhedral. Fresh olivine is observed in the less altered interiors of some pieces, but, in most cases, it is totally replaced by Fe oxyhydroxides + clay (see **"Alteration,"** p. 8).

Groundmass textures are microcrystalline, ranging from intersertal to various quench morphologies (e.g., sheaf and plumose) close to chilled margins. Acicular to skeletal plagioclase forms ~20% of the groundmass. However, in contrast to Type 1 basalts, groundmass olivine is not present in the one available thin section (Sample 3R-1, 107–108). Fe-Ti oxides occur as minute (<10 µm) equant crystals and make up ~1% of the groundmass. Dark brown, quench-textured mesostasis constitutes 50%–75% of the rock. Small spherical vesicles (<200 µm in diameter) are filled with clay ± Fe oxyhydroxides in alteration halos but can be unfilled in less altered portions of the rock (see **"Alteration,"** p. 8).

F4. Spinel microphenocryst containing melt inclusions, p. 16.

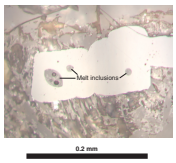

F5. Miarolitic cavity in a moderately plagioclase-olivine phyric Type 1 basalt, p. 17.

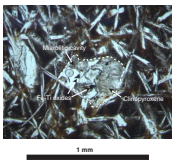

Aphyric Basalt (Type 3). Type 3 basalts are distinguished from Type 2 basalts by being fine grained as opposed to being microcrystalline (Table T2). They consist of <1% prismatic to tabular plagioclase microphenocrysts (1–2 mm) (Fig. F3), and rare olivine microphenocrysts (<1 mm) in a subophitic to intergranular groundmass (Fig. F6). The groundmass consists of ~45% subhedral to anhedral plagioclase and ~35% anhedral clinopyroxene. Most plagioclase crystals are normally zoned, but some microphenocrysts and larger groundmass crystals show discontinuous zoning. Alteration to a birefringent clay mineral commonly occurs along discontinuous, subparallel microcracks (Fig. F7). Although now totally replaced by Fe oxyhydroxides + clay (iddingsite), equant olivine crystals (0.1–0.3 mm) originally composed ~15% of the rock (Fig. F6). Fe-Ti oxide minerals range from equant to elongate shapes that fill interstitial areas between silicate minerals and are as large as 300 µm.

Chilled Margins. Chilled margins were recovered on 14 of the rubble clasts (i.e., 17% of the pieces). Only one chilled margin was recovered on a Type 2 basalt (Sample 3R-2 [Piece 18]); the remainder are on Type 1 basalts. Few of the pieces retain a significant thickness of clear glass, and most consist of glass plus spherulitic quench crystals heavily altered to palagonite. In one case the chilled margin appears to be partially replaced by blue cryptocrystalline silica and/or clay? (see "Alteration," p. 8). Sample 3R-1 (Piece 12) is an exception, consisting of <1 mm of palagonite and 4–5 mm of clear glass + phenocrysts (Fig. F8). The zone of coalesced spherulites is relatively thin (3–4 mm), and the spherulites are small (~100–200 µm in diameter). The entire sequence of chilled margin textures (i.e., spherulitic to quench plumose and sheaf morphologies) extends for >3 cm into the interior of the piece. This sequence of quench textures is typical of those observed in the other, albeit more altered, samples with chilled margins from this hole.

Petrography of the Breccia

There are several breccia intervals in Unit 1 of Hole 1161A: Section 3R-2 (Pieces 7, 8, and 11), Section 4R-1 (Pieces 9–12), and Section 5R-1 (Pieces 11–14 and 17). The breccias are poorly sorted (Fig. F9); sorting by size or density is not apparent. Clast sizes range from small pebbles (<4 cm) to coarse sand (<1 mm). Only clasts of basaltic derivation are visible in the breccia; included are basalt, palagonite ± glass ± spherulites, olivine (rare), and plagioclase. Whether individual basaltic clasts are derived from aphyric or phyric basalt is difficult to determine because of their small size (basalt clasts as small as 100 µm are readily identifiable) and, in some cases, their high degree of alteration (see "Alteration," p. 8). However, larger aphyric and phyric basalt clasts are clearly identical to the microcrystalline Type 1 and Type 2 basalts described in detail above. Fine-grained aphyric basalt (Type 3), however, has not been identified as clasts in the breccia.

Approximately 15% of the sand-sized clasts are angular plagioclase crystals (Fig. F10). Most of these are unaltered, but some are altered to a birefringent material along microcracks (Fig. F11). This alteration style is similar to that of the plagioclase crystals in the fine-grained aphyric basalts (see Fig. F7), suggesting that some feldspars may be derived from Type 3 basalts.

Basaltic clasts are typically angular, whereas palagonite ± glass clasts are angular to subrounded; the latter commonly show concentric layers of different colors that parallel the shape of the piece (Fig. F9). This suggests that at least some of the alteration occurred within the breccia

F6. Subophitic to intergranular groundmass texture typical of fine-grained aphyric basalt, p. 18.

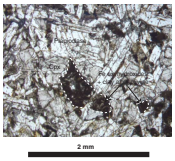

F7. Alteration of plagioclase to sericite? along microcracks, p. 19.

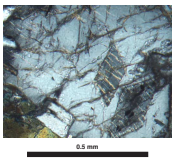

F8. A sequence of chilled margin textures typical of moderately plagioclase-olivine phyric basalt, p. 20.

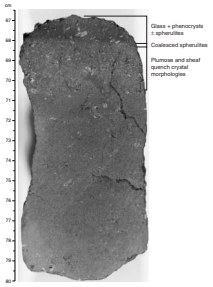

F9. A basaltic breccia typical of Hole 1161A, p. 21.

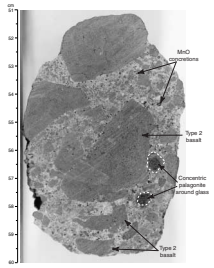

F10. Photomicrograph of basaltic breccia matrix, p. 22.

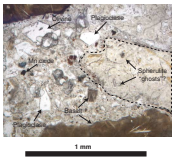

rather than before deposition (see "Alteration," p. 8). Basalt dominates among the clasts larger than ~5 mm, but palagonite and basalt are present in roughly equal abundance in the very coarse sand to granule size range (i.e., 1–4 mm).

The matrix material between the breccia clasts is a cream to white clayey silt, most of which comes from the breakdown of highly altered material derived from basaltic chilled margins. Clasts that were originally composed of glass ± spherulites are now composed of pale yellow to buff-colored clay; "ghosts" of spherulites and plagioclase microlites can still be observed (Fig. F10). Although some of these clay pseudomorphs retain original clast outlines, others are partially disaggregated, and these appear to be the main source of interstitial clay matrix for the breccia. Similarly, a single crystal of unaltered olivine was observed in the breccia matrix in Sample 187-1161A-4R-1, 65–68 cm, adjacent to a moderately plagioclase-olivine phyric basalt clast (Fig. F10). The fact that olivine crystals are relatively rare in the breccia matrix, by comparison with plagioclase, suggests that in most cases the olivine has been quickly broken down into clay minerals and incorporated into the finer grained matrix.

The matrix is loosely cemented by thin (~10 µm) selvages of cryptocrystalline silica and/or clay that surround the clasts (Figs. F11, F12A); locally it is cemented by crystalline quartz (e.g., Section 187-1161A-4R-1). Mn oxide lines the edges of some pore spaces between clasts, adjacent to the silica cement (Fig. F12B). Patches of Mn-Fe oxyhydroxides and Mn oxide concretions also are present throughout the matrix (Fig. F10). Minor amounts of calcite were detected by the reaction of the core pieces with dilute HCl (~5%–10%) in a few places in Section 187-1161A-5R-1. Whether this was due to the presence of a calcareous sediment or to local precipitation of a calcite cement was impossible to determine because of the fine-grained nature of the matrix.

F11. Photomicrograph of basaltic breccia matrix, p. 23.

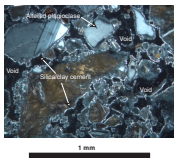

F12. Photomicrograph of basalt breccia matrix, p. 24.

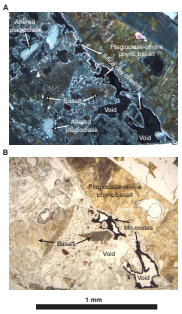

Hole 1161B

Unit 1

Petrography of Basalts

Similar to Hole 1161A, Unit 1 of Hole 1161B consists of basaltic rubble with several intervals of basaltic breccia: Section 187-1161B-1W-1 (Pieces 3–6) and Section 187-1161B-2R-1 (Pieces 2–4, 9). Four different igneous lithologies occur among the rubble clasts. Three of these are identical to the basalts in Hole 1161A, i.e., Types 1, 2, and 3 (Table T2). The fourth lithology in Hole 1161B (Type 4) is aphyric basalt, distinguished from Type 3 aphyric basalt by its medium gray color and microcrystalline groundmass texture (Table T2; Fig. F13). Types 1, 2, and 4 basalts are observed as clasts within the breccias in Hole 1161B; the fine-grained aphyric basalt (Type 3) is not.

The four types of basalt clast are intermixed throughout the hole, but Type 4 aphyric basalt predominates, constituting 47% of the recovered rubble clasts. Types 1 and 2 basalts occur in equal proportions (i.e., 23%), whereas Type 3 fine-grained aphyric basalt makes up only 7% of the clasts. Types 1 and 2 basalts range from moderately to highly altered. In highly altered clasts, the alteration is characterized by pervasive replacement of olivine and groundmass by a mixture of Fe oxyhydroxides and clay; in moderately altered pieces, a similar type of oxidative alteration is concentrated in halos that have formed adjacent to veins, fractures, and outer weathered surfaces. Type 4 aphyric basalts

F13. Microcrystalline aphyric basalt (Type 4), p. 25.

are slightly to moderately altered, with alteration restricted to relatively narrow alteration halos along edges of pieces and around fractures (see "Alteration," p. 8). No thin sections were made of basalts from Hole 1161B, so only macroscopic observations are provided below. However, at this level of examination, Types 1, 2, and 3 basalts are virtually indistinguishable between the two holes. Only a few differences were noted:

1. One Type 1 basalt in Hole 1161B is highly phyric (Sample 187-1161B-3R-1 [Piece 3]; Fig. F14) rather than moderately phyric. It contains ~4% equant olivine and ~8% tabular to prismatic plagioclase phenocrysts. The phenocrysts are slightly larger, on average, than in other Type 1 basalts, with plagioclase crystals up to 8 mm long and equant olivines as large as 4 mm.
2. Small (<0.2 mm) spherical vesicles occur in the Type 2 basalts in Hole 1161B and constitute <1% of the rock. These are filled with a yellowish-green clay ± Mn oxide in altered areas but elsewhere are unfilled (see "Alteration," p. 8). Miarolitic cavities up to 1.5 mm across were also identified in one piece, Sample 187-1161B-2R-1 (Piece 10).
3. Rare (<<1%) spherical vesicles as large as 1 mm in diameter were observed in one Type 3 basalt (Sample 187-1161B-1W-1 [Piece 11]); these are concentrated on one side of the piece and filled with yellow to green smectite.

Microcrystalline Aphyric Basalt (Type 4). The microcrystalline aphyric basalt is medium gray. It is devoid of phenocrysts, although small, sparse, olivine microphenocrysts are present throughout. Spherical vesicles form ~1% of the rock and range from unfilled to lined or filled with calcite or green to white clay or blue cryptocrystalline silica.

Chilled Margins. Chilled margins were recovered on three rubble clasts (10% of the pieces); one is Type 2 phyric basalt and two are Type 4 aphyric basalts. None of the pieces retain a significant thickness of clear glass—they consist of partially palagonitized glass plus spherulitic quench crystals (see "Alteration," p. 8). The spherulites are small (<0.2 mm) in all cases.

Petrography of the Breccia

Basaltic breccia occurs in several intervals in Unit 1 of Hole 1161B: Section 1W-1 (Pieces 3–6) and Section 2R-1 (Pieces 2–4, 9). The breccias are similar to those recovered in Hole 1161A (Figs. F15, F16, F17, F18), with only a few differences:

1. Type 4 aphyric basalt clasts are common in the breccias in Hole 1161B, in addition to Type 1 and Type 2 phyric basalts (Fig. F15). Chilled margins occur on clasts of all basalt types among the breccia clasts (Figs. F16, F17).
2. The maximum clast size is slightly smaller (<2.5 cm in Hole 1161B, ~4 cm in Hole 1161A).
3. Basalt clasts in the breccias of Hole 1161B show a wider range of alteration characteristics, pervasively altered basalt, basalt with clay, and/or palagonite alteration halos, and/or clay pseudomorphs after basalt clasts (Figs. F15, F17) (see "Alteration," p. 8). As in Hole 1161A, spherulitic textures are still visible in the clay pseudomorphs of basalt chilled margin clasts (Fig. F18).
4. As in Hole 1161A, basalt dominates among the pebble-sized clasts, and palagonite and basalt are present in roughly equal

F14. Plagioclase-olivine phyric basalt (Type 1), p. 26.

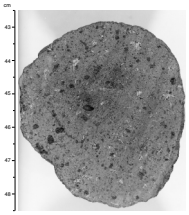

F15. Basalt breccia with a range of alteration characteristics in the basalt clasts, p. 27.

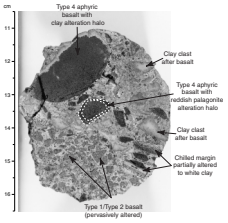

F16. Basalt breccia in which the proportions of clast types vary, p. 28.

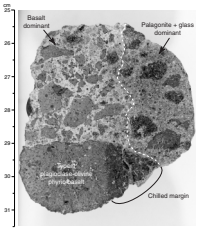

F17. Basalt breccia showing palagonitized chilled margin in basalt clast, p. 29.

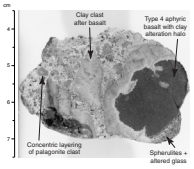

F18. Photomicrograph of a basalt chilled margin clast, totally replaced by clay, p. 30.

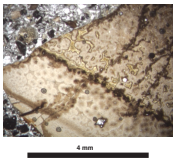

proportions in the very coarse sand to granule-size range. However, in Section 187-1161B-1W-1, palagonite ± glass dominates the 1- to 2-mm-size clast range. Sample 187-1161B-1W-1, 16–21 cm, for example, is made up entirely of palagonite + glass fragments (Fig. F19). However, this is not a hyaloclastite, since a contact between this breccia type and one containing predominantly basalt clasts is seen in interval 187-1161B-1W-1, 25–31 cm (Fig. F16). In addition, clasts showing a range of alteration characteristics are found in the same piece (Fig. F15). The latter suggests a multistage alteration history for some of the basalt clasts; some of that alteration must have occurred prior to breccia formation (see "Alteration," p. 8).

5. The matrix material between breccia clasts is similar in Holes 1161A and 1161B, being a cream to white clayey silt composed of highly altered material derived from basaltic chilled margins. However, Hole 1161B matrix material is cemented by a greater range of silica types (i.e., white to blue-gray cryptocrystalline material to drusy or euhedral clear quartz). Botryoidal to euhedral quartz is also observed filling vugs and pore spaces (e.g., Section 187-1161B-2R-1).

F19. Palagonite + glass–rich breccia, p. 31.

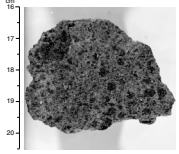

ALTERATION

Mixed basaltic rubble and basalt breccia were recovered from Holes 1161A and 1161B (see "Igneous Petrology," p. 3). Basaltic rubble and basaltic clasts in the breccia from both holes are moderately to highly altered by low-temperature reactions.

F20. Basaltic breccia, p. 32.

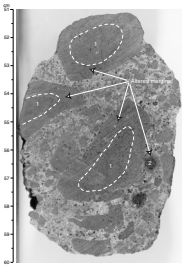

Basaltic Breccia

In the breccia from Hole 1161A, most of the pebble-sized (~2–4 cm) basalt clasts have altered margins from 5 to 10 mm wide, whereas smaller clasts (<0.1–1 cm) are altered throughout (Fig. F20). The alteration of the basalt clasts is characterized by partial to complete replacement of olivine and pyroxene by Fe oxyhydroxides and brown clay. A thin layer of Mn oxide commonly encircles the clasts, and Mn oxide dendrites occasionally penetrate several millimeters into the interior. Clasts of glassy pillow margin material are partially to completely altered to palagonite. The palagonite typically forms concentric layers of varying colors, mimicking the shape of the clasts. As all clasts have unbroken altered margins, alteration most likely occurred after deposition.

F21. Basaltic breccias with thin silica and clay layers surrounding basaltic clasts, and Mn oxide lining voids, p. 33.

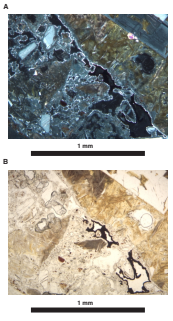

Plagioclase clasts are usually fresh, but some have a birefringent material along internal microcracks. The cream to white clayey silt matrix between the clasts consists mainly of completely altered, disaggregated material from chilled margins. The clasts are surrounded by thin (~10 µm) selvages of cryptocrystalline silica and/or clay (Fig. F21A). Patches of Fe oxyhydroxide and Mn oxide are distributed randomly throughout the matrix, occasionally lining or filling spaces between clasts (Fig. F21B). Locally, quartz and calcite are present in the matrix. Because of the fine-grained nature of the matrix, it is unclear whether the calcite is a sediment infill or has precipitated within the deposit.

F22. Highly altered glassy clast in breccia, p. 34.

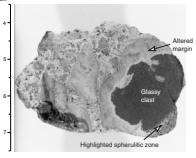

In the breccia from Hole 1161B, most of the pebble-sized (<1–4 cm) clasts have altered margins from 1 to 5 mm wide (Fig. F22). The altered margins as well as smaller clasts (<0.1–1.5 cm) of both basalt and chilled margins are frequently completely replaced by light brown to gray clay

(Figs. F18, F23, F24). In some glassy clasts, the outer margins consist of reddish palagonite. Clasts with both types of alteration margins are also present. Quartz is more abundant than in cores from Hole 1161B than cores from Hole 1161A.

Basaltic Rubble

In basalt from Hole 1161A, the fracture plus vein density ranges from 3.2/m to 10.7/m and averages 8.3/m. Rare veins are present in Sections 187-1161A-3R-1 and 3R-2. The vein density from Hole 1161A averages 0.6/m, and the calculated volume percent of veins averages 0.02. In basalts from Hole 1161B, the fracture plus vein density ranges from 6.0/m to 11.8/m and averages 8.1/m. Veins were only noted in Core 187-1161B-3R. The vein density from Hole 1161B averages 2.3/m, and the calculated volume percent of veins averages 0.03. The fractures and veins are usually coated or filled with Mn oxide or silica in cores from both holes. In pervasively altered pieces, there are no distinct alteration halos along fractures and veins. In moderately altered pieces, however, alteration halos up to 1 cm wide are occasionally present. Alteration along fractures through chilled margins highlights a 1- to 2-cm zone of large coalesced spherulites in several pieces (Fig. F25). Rare cavities (<3 mm wide) are unfilled to partially filled with clay and Mn oxide or lined with blue silica, quartz, Mn oxide, and occasionally with unidentified gray to orange platy crystals (Section 187-1161A-4R-1 [Piece 3]). Vesicles are unfilled or lined to filled with yellow to green clay ± blue silica ± calcite.

In moderately altered pieces the alteration is strongest within 5- to 25-mm-wide halos along outer edges (Fig. F26) and within the inner parts of chilled margins with large coalesced spherulites (Fig. F25). Pieces with pervasive alteration are common in both holes. The surfaces of pieces are commonly coated with cream-colored silty sediment with Mn oxide concretions and yellow fragments of palagonite (e.g., Section 187-1161A-3R-1) ± clay ± calcite ± quartz. Some pieces have dendritic growth of Mn oxide penetrating ~3 mm into the interior. Glassy margins are usually heavily altered to yellow-brown palagonite. In Section 187-1161A-3R-1 (Piece 18), however, the glass is partially replaced by bluish clay and possibly silica (Fig. F27).

The alteration halos are characterized by partial to complete replacement of olivine phenocrysts and groundmass olivine and pyroxene by Fe oxyhydroxides and brown clay. Occasionally pieces with some unaltered olivine are present (e.g., Section 187-1161A-3R-1 [Pieces 12 and 14]). Plagioclase phenocrysts are unaltered to partially Fe stained throughout. Small primary sulfide globules and larger single composite grains of pyrite, chalcopyrite, magnetite, and hematite are occasionally present (e.g., Section 187-1161A-2R-1) (Fig. F28). Due to the interstitial occurrence within other phases and an irregular morphology, the larger composite grains are probably secondary.

MICROBIOLOGY

Two rock samples were collected at Site 1161 as soon as the core liners were split to characterize the microbial community inhabiting this environment (Table T3). One sample is a breccia fragment (Sample 187-1161A-4R-1 [Piece 10, 57–60 cm]), and one is a pillow basalt fragment composed of partially altered glass rind and crystalline basalt interior

F23. Radial clay aggregates replacing spherulites, p. 35.

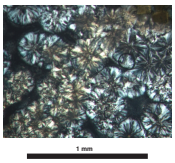

F24. Clast of yellow palagonite partially replaced by light brown clay, p. 36.

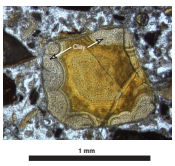

F25. Fractures lined with bluish cryptocrystalline silica within chilled margin of pillow fragment, p. 37.

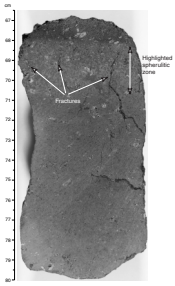

F26. Basaltic clast with an alteration halo around outer edges, p. 38.

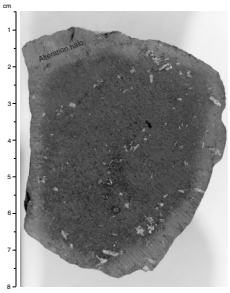

(Sample 187-1161A-3R-1 [Piece 24, 141–143 cm]). To sterilize them, the outer surfaces of the rocks were quickly flamed with an acetylene torch, and enrichment cultures and samples for DNA analysis and electron microscope studies were prepared (see "Igneous Rocks," p. 7, in "Microbiology" in the "Explanatory Notes" chapter).

SITE GEOPHYSICS

Site location for Site 1161 was based on a Leg 187 single-channel seismic survey conducted during the transit from Site 1158 to Site 1159 (*JOIDES Resolution* survey line S7; Fig. F13, p. 19, in the "Site 1159" chapter). The roughly north-south seismic profile between shotpoints 1074 and 1283 shows a ~1.6-km-wide basin structure, centered near shotpoint 1205 (see site AAD-38a in Fig. F15, p. 21, in the "Site 1159" chapter). The proposed site (AAD-38a) is near shotpoint 1200, located slightly toward the northern side of the basin.

An additional 0.9-hr 3.5-kHz PDR survey was conducted on approaching the site. Because of an unknown navigation problem, the apparent position of the basin structure was found to be shifted ~1 km northward relative to the position derived from the seismic profile. Hole 1161A, ~0.5 km north of the proposed site, is in a location corresponding to shotpoint 1216 of the S7 seismic profile. Sediment cover at this position is from 6.77 to 6.87 s two-way traveltime, equivalent to at least 100 m of sediment (see Fig. F15, p. 21, in the "Site 1159" chapter). Before basement was reached, we washed through 116 m of sediment in Hole 1161A, whereas about 220 m to the north in Hole 1161B, we penetrated 158.5 m sediment. Both thicknesses are consistent with estimates from the seismic profile.

SEDIMENTS

A single wash barrel containing a slurry of drilling-induced clay pellets was recovered from Hole 1161A. The pellets range from submillimeter to 2 mm in size, and the sediment is poorly sorted but normally graded as a result of agitation in the core barrel. The sediment is a mixture of medium brown and medium dark brown siliceous clay with no calcareous component. The upper 4 cm of Section 187-1161A-1W-CC is comprised of fragments, up to 2 cm, of severely drilling-disturbed, densely packed, medium brown and medium dark brown siliceous clay. Five small pieces of basalt were recovered from the bottom of the core catcher.

No sediment was recovered in the wash barrel from Hole 1161B.

GEOCHEMISTRY

Introduction

At Site 1161, basaltic samples were recovered from two holes, 1161A and 1161B. The site is located in Zone A, 43 km south of Site 1158, on ~19-Ma crust that we interpret to be within the transferred lithosphere domain of an extinct westward-propagating rift. This site was selected to test whether Indian- or Pacific-type mantle was present during the

F27. Replacement of shiny black glass by bluish clay and silica, p. 39.

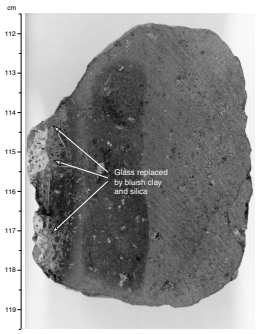

F28. Composite secondary pyrite, chalcopyrite, magnetite, and hematite, p. 40.

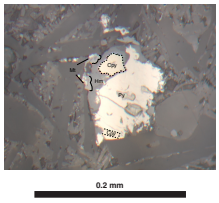

T3. Rock samples for cultures, DNA analysis, SEM/TEM, and contamination studies, p. 46.

waning stages of magmatism that resulted from abandonment by rift propagation.

In Hole 1161A we encountered a single lithologic unit of basaltic rubble with intervals of basaltic breccia. From Hole 1161B we recovered similar material that was likewise assigned to a single lithologic unit. One glass sample was removed from a breccia clast in Hole 1161A and analyzed for major and trace elements by ICP-AES, and one aphyric basalt whole-rock sample from Hole 1161A was analyzed for major and trace elements by XRF (Table T4). No samples from Hole 1161B were analyzed.

T4. Compositions of basalts, Site 1161, p. 47.

Hole 1161A

The Site 1161A glass has a relatively unfractionated composition (i.e., ~8.0 wt% MgO) with characteristics typical of Zone A lavas (Figs. F29, F30). The Hole 1161A whole rock contains less MgO than the glass and exhibits the same characteristics that suggest loss of Mg by alteration in whole-rock samples from every Leg 187 site. This conclusion is supported by thin-section examination of whole-rock Sample 187-1161A-4R-1, 105–109 cm (Fig. F7), which shows high degrees of alteration; not unexpectedly, a relatively high loss on ignition (1.44 wt%) was measured on this sample.

F29. Major element compositions vs. MgO for Hole 1161A basalts, p. 41.

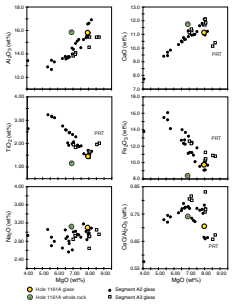

F30. Trace element compositions vs. MgO for Hole 1161A basalts, p. 42.

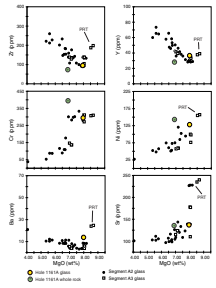

Temporal Variations

The glass is compositionally similar to unfractionated lavas dredged from Southeast Indian Ridge (SEIR) Segments A2 and A3. The high Ba and Sr and low CaO/Al_2O_3 ratios suggest a low degree of melting. The Hole 1161A glass composition plots near lavas recovered from the rift tip region of segments undergoing propagation (e.g., Ba, Y, and CaO/Al_2O_3), suggesting, as inferred from the seafloor terrain and magnetic anomaly offsets (Vogt et al., 1984), an association with the propagating rift tip tectonic environment.

Mantle Domain

The Zr/Ba systematics of Hole 1161A basaltic glass indicate an Indian-type mantle source, as the sample plots within the Indian-type mid-ocean-ridge basalt field in Figure F31. Even though the glass sample plots on the Pacific side of the Na_2O/TiO_2 vs. MgO diagram, the data are nonetheless consistent with an Indian mantle provenance since the glass overlaps the compositions of transitional Segment B5 axial lavas. Furthermore, Leg 187 Na_2O/TiO_2 vs. MgO relationships are consistently offset to lower Na_2O/TiO_2 values relative to zero-age SEIR basalt glass (see "Sodium and Titanium," p. 13, in the "Leg Summary" chapter). Hole 1161A glass has high Na_2O/TiO_2 relative to other Leg 187 compositions and is therefore Indian type in composition. From these data, Site 1161 lavas appear to document another incursion of Indian-type mantle east of the AAD/Zone A transform boundary.

F31. Variations of Zr/Ba vs. Ba and Na_2O/TiO_2 vs. MgO for Hole 1161A basaltic glass and whole-rock samples, p. 43.

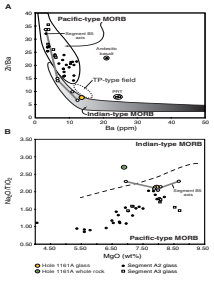

REFERENCE

Vogt, P.R., Cherkis, N.K., and Morgan, G.A., 1984. Project Investigator—1. Evolution of the Australian-Antarctic Discordance from a detailed aeromagnetic study. *In* Oliver, R.L., James, P.R., and Jago, J. (Eds.), *Antarctic Earth Science*. Proc. 4th Internat. Symp. Antarctic Earth Sci.: Canberra (Aust. Acad. Sci.).

Figure F1. Photograph of interval 187-1161A-4R-1, 36–43 cm, showing a moderately plagioclase-olivine phyric basalt typical of Hole 1161A, Type 1.

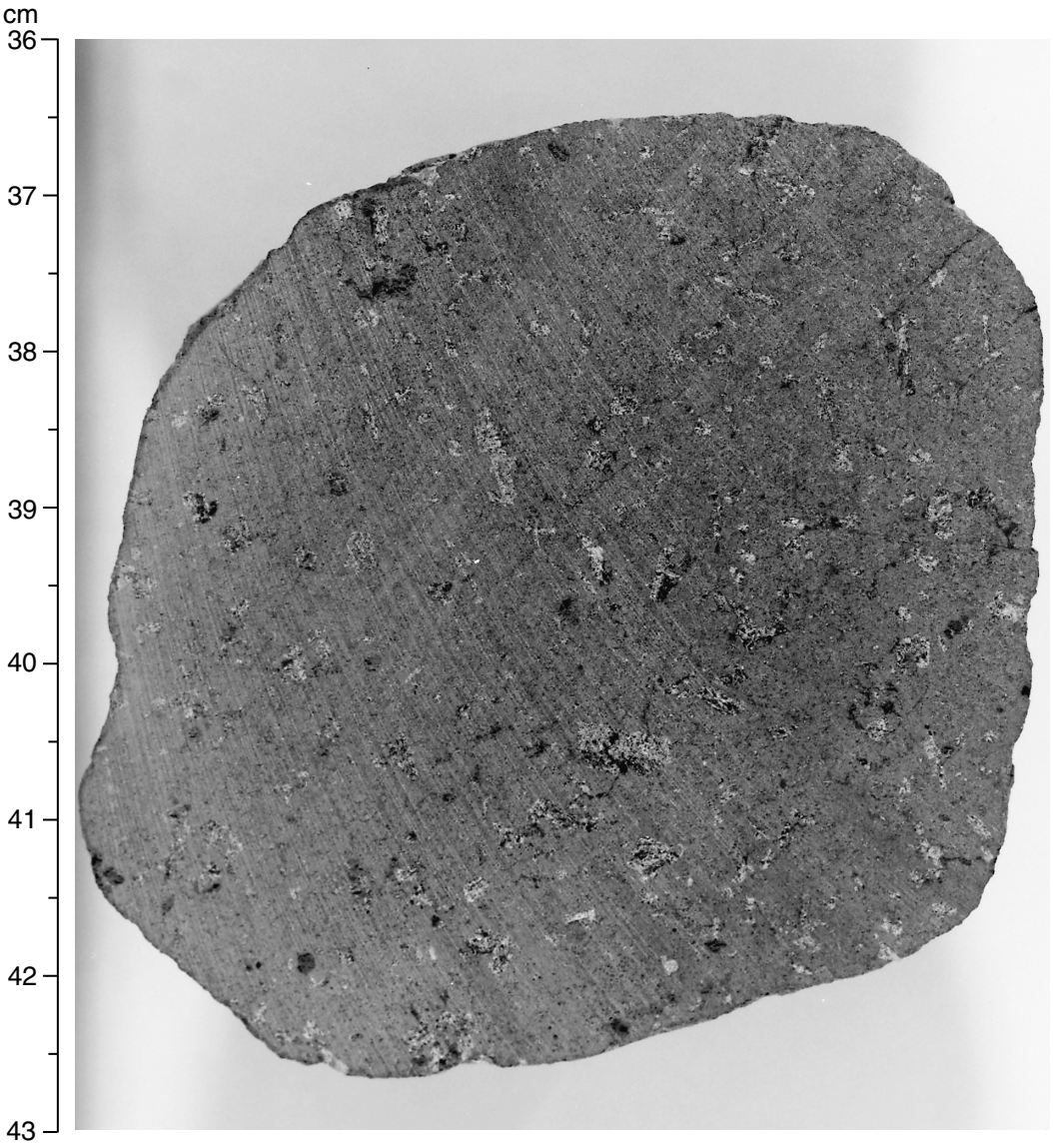

Figure F2. Photograph of interval 187-1161A-3R-1, 15–21 cm, showing an aphyric to sparsely plagioclase ± olivine phyric basalt typical of Hole 1161A, Type 2.

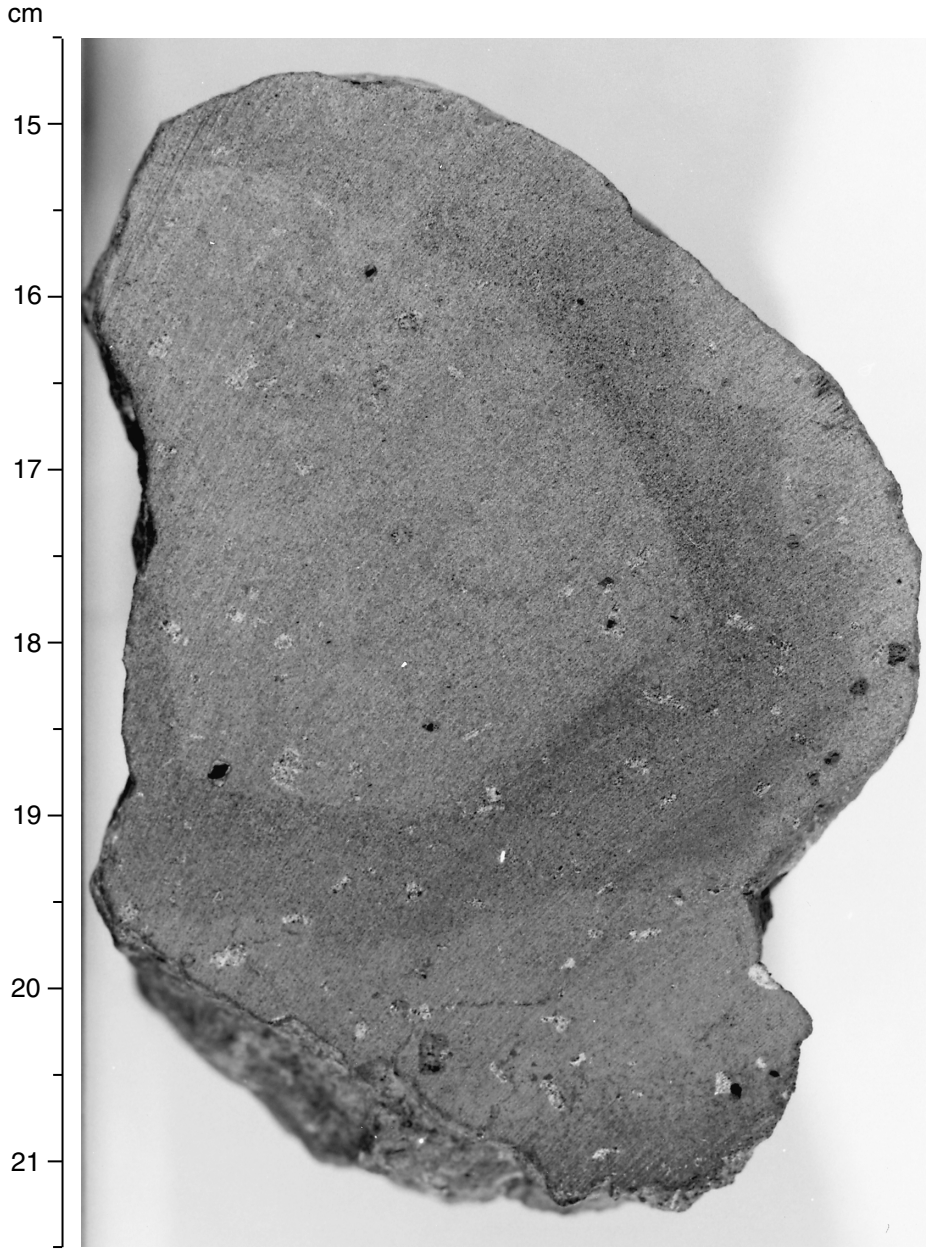

Figure F3. Photograph of interval 187-1161A-4R-1, 80–89 cm, showing a fine-grained aphyric basalt typical of Hole 1161A, Type 3. Note the rare plagioclase and olivine microphenocrysts between 87 and 88 cm.

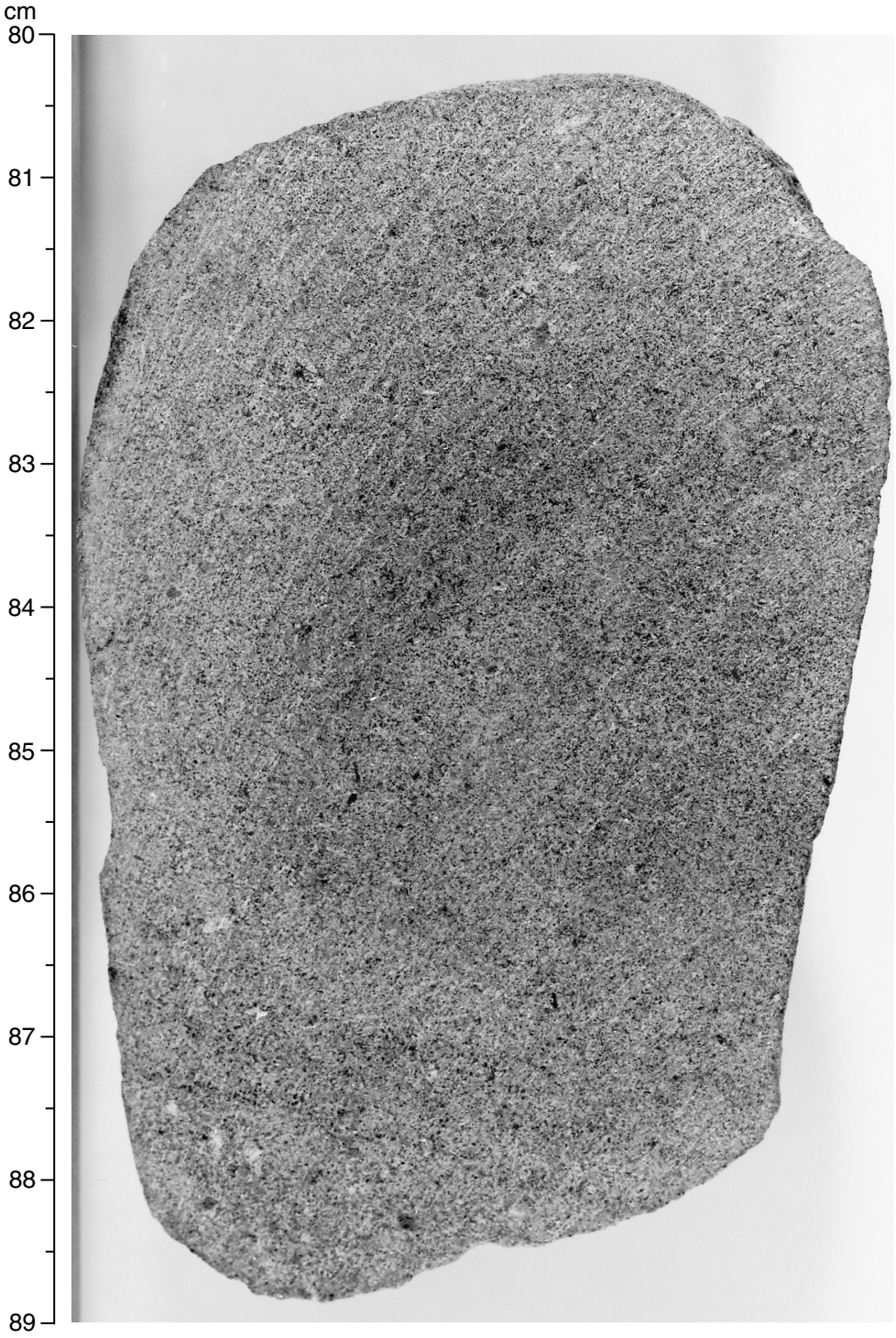

Figure F4. Photomicrograph in reflected light of Sample 187-1161A-2R-1, 10–13 cm (see **"Site 1161 Thin Sections,"** p. 16), showing a spinel microphenocryst containing melt inclusions in a moderately plagioclase-olivine phyric Type 1 basalt.

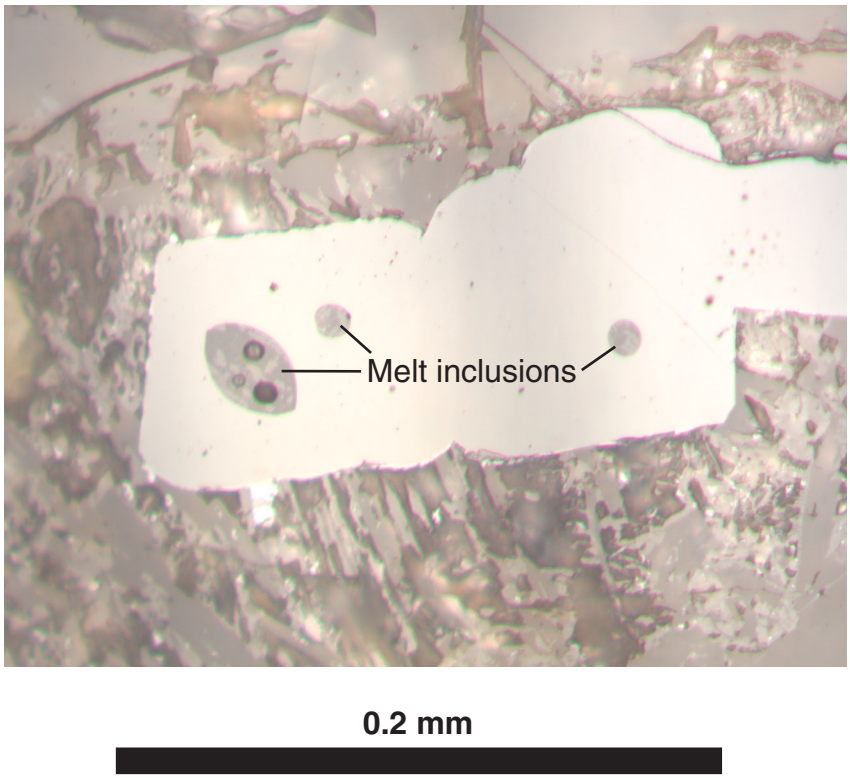

Figure F5. Photomicrograph in plane-polarized light of Sample 187-1161A-2R-1, 10–13 cm (see **"Site 1161 Thin Sections,"** p. 16), showing clinopyroxene and Fe-Ti oxide in a miarolitic cavity in a moderately plagioclase-olivine phyric Type 1 basalt. Intersertal groundmass textures in the surrounding areas are typical for this basalt type.

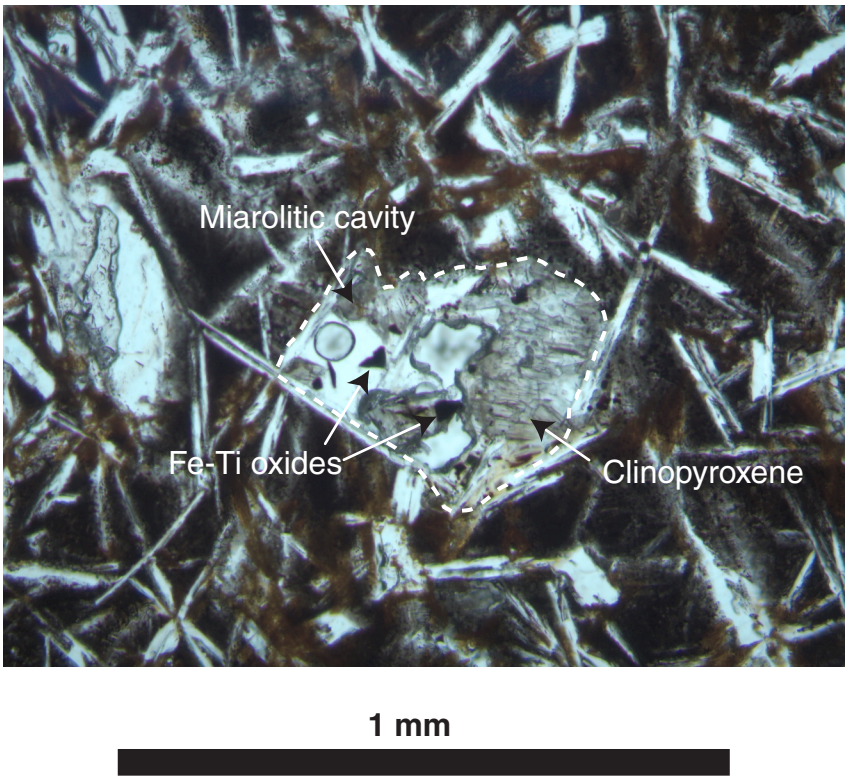

Figure F6. Photomicrograph in plane-polarized light of Sample 187-1161A-4R-1, 105–109 cm (see "Site 1161 Thin Sections," p. 20), showing subophitic to intergranular groundmass texture typical of Type 3 fine-grained aphyric basalt. Olivine microphenocryst and groundmass crystals are totally replaced by Fe oxyhydroxides + clay. Cpx = clinopyroxene.

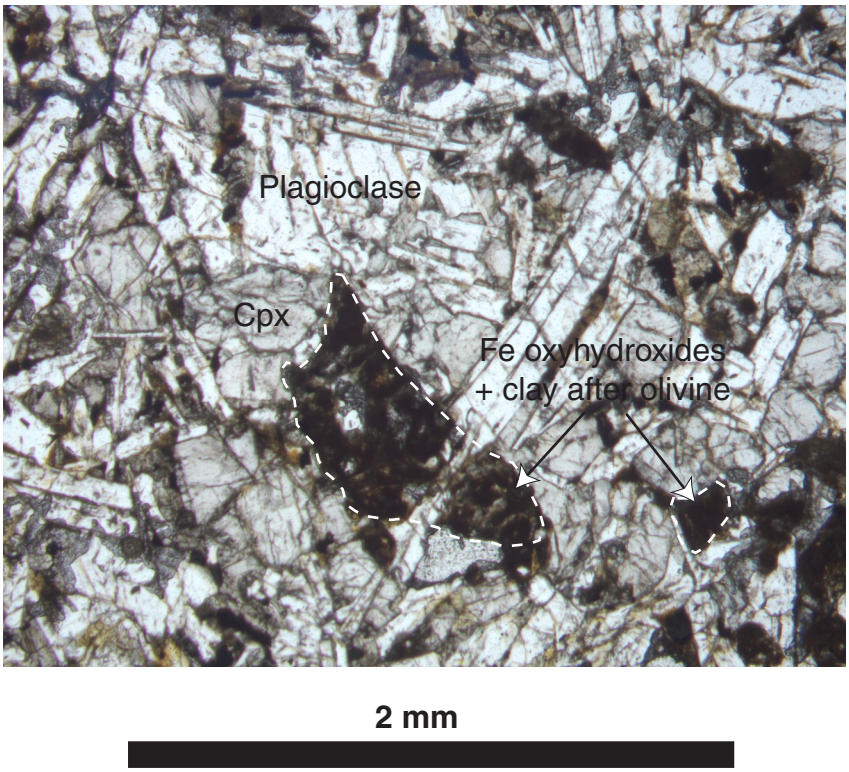

Figure F7. Photomicrograph of Sample 187-1161A-4R-1, 105–109 cm (see **"Site 1161 Thin Sections,"** p. 20), showing alteration of plagioclase to sericite? along microcracks.

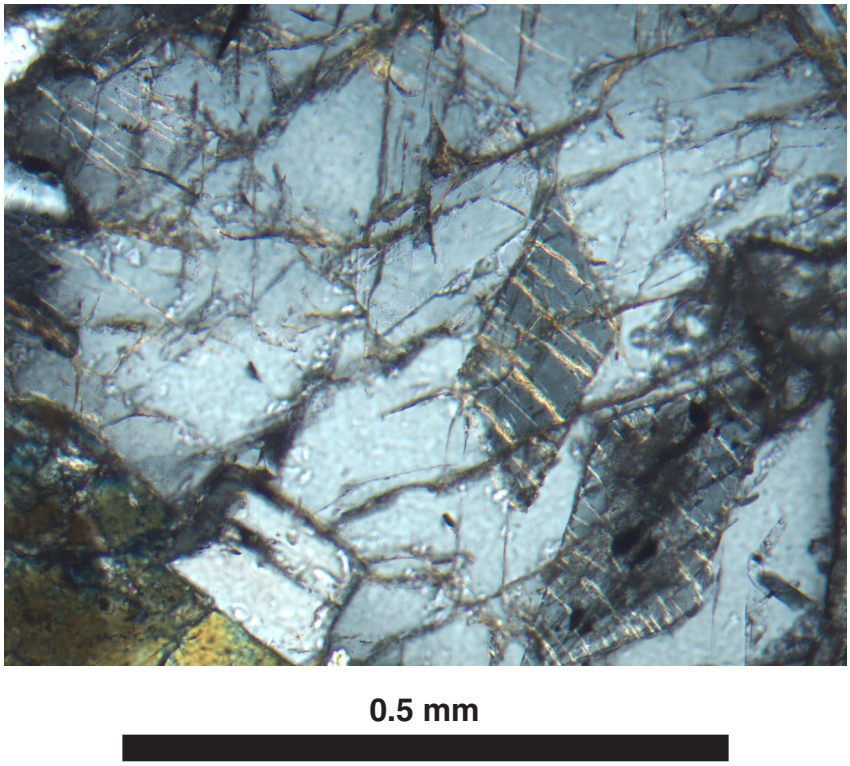

Figure F8. Photograph of interval 1161A-3R-1, 67–80 cm, showing a sequence of chilled margin textures typical of moderately plagioclase-olivine phyric basalt.

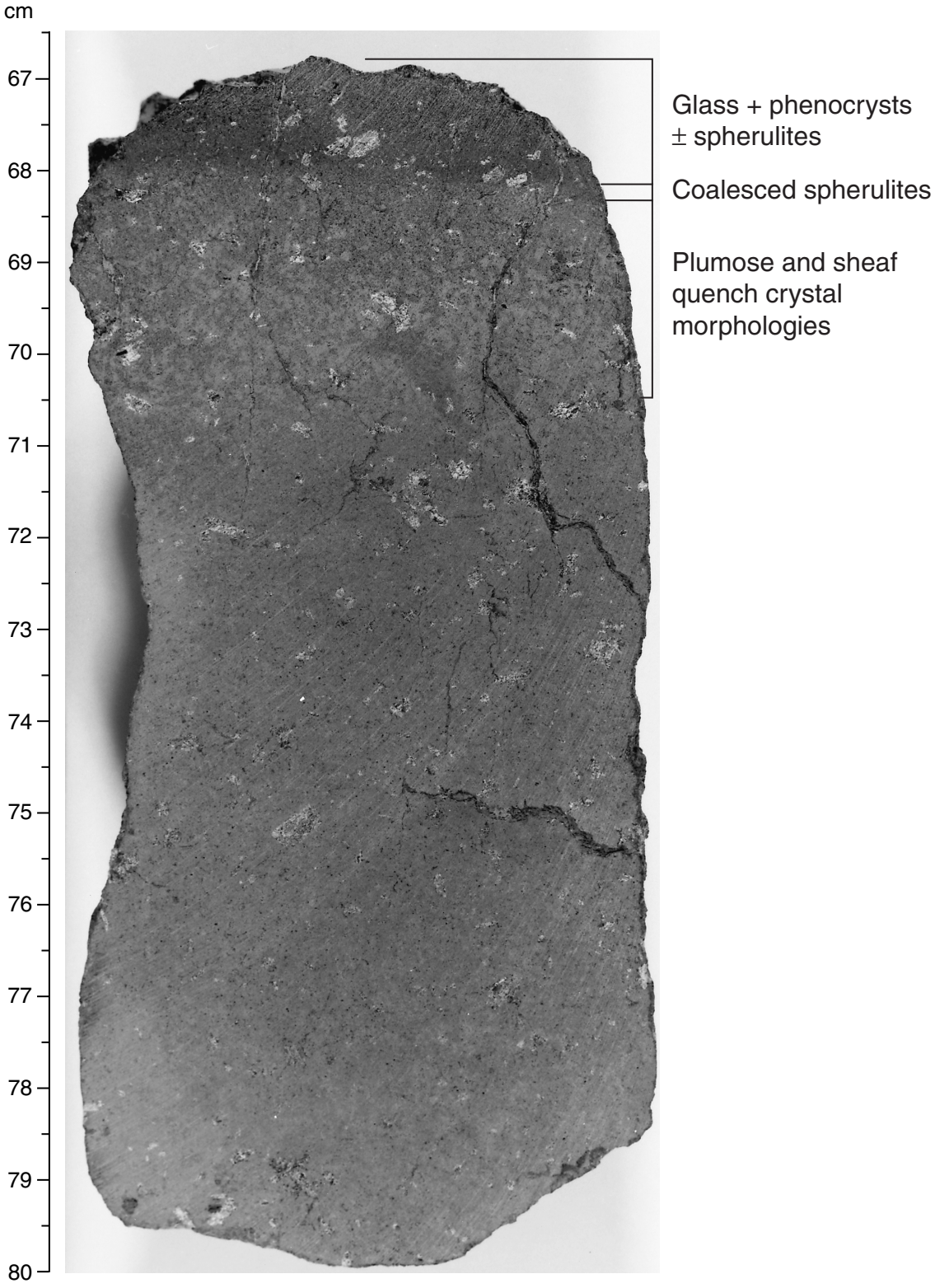

Figure F9. Photograph of interval 187-1161A-5R-1, 51–60, showing a basaltic breccia typical of Hole 1161A.

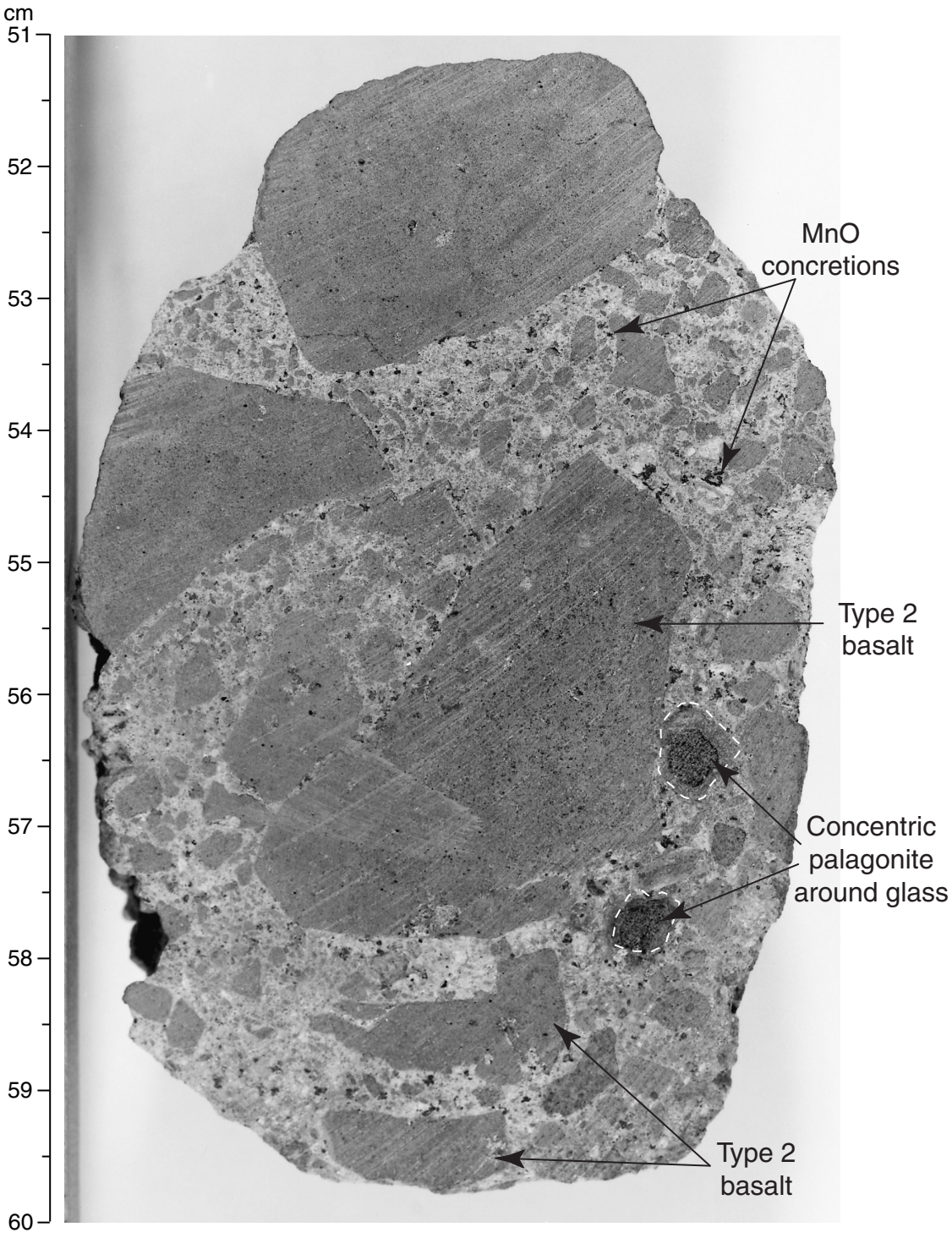

Figure F10. Photomicrograph in plane-polarized light of Sample 187-1161A-4R-1, 65–68 cm (see "Site 1161 Thin Sections," p. 19), showing angular feldspar clasts and a chilled margin fragment (now totally altered to clay minerals) within basalt breccia matrix. Note the presence of Mn oxide concretions and small (sand-sized) basalt clasts.

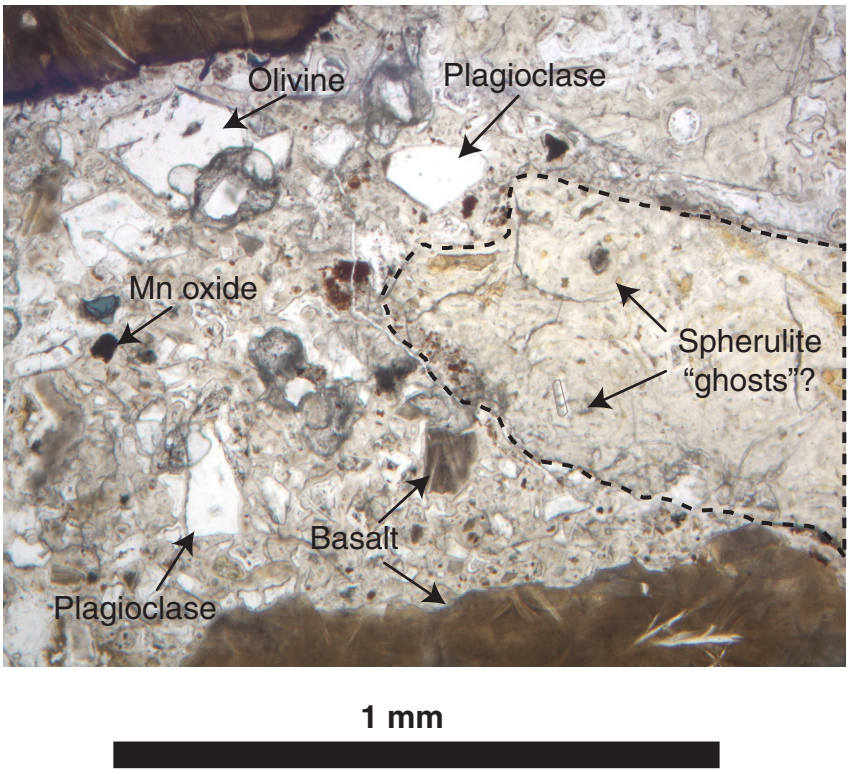

Figure F11. Photomicrograph, with crossed polars, of Sample 187-1161A-4R-1, 65–68 cm (see **"Site 1161 Thin Sections,"** p. 19), showing clasts loosely cemented by cryptocrystalline silica and/or clay (birefringent material outlining clasts) in basalt breccia matrix. Note the angular shapes and abundance of feldspar clasts. Partial alteration of some plagioclase crystals along discontinuous, parallel microcracks is similar to the alteration style of plagioclase in the fine-grained aphyric basalt. This suggests that at least some of the feldspars are derived from this lithology.

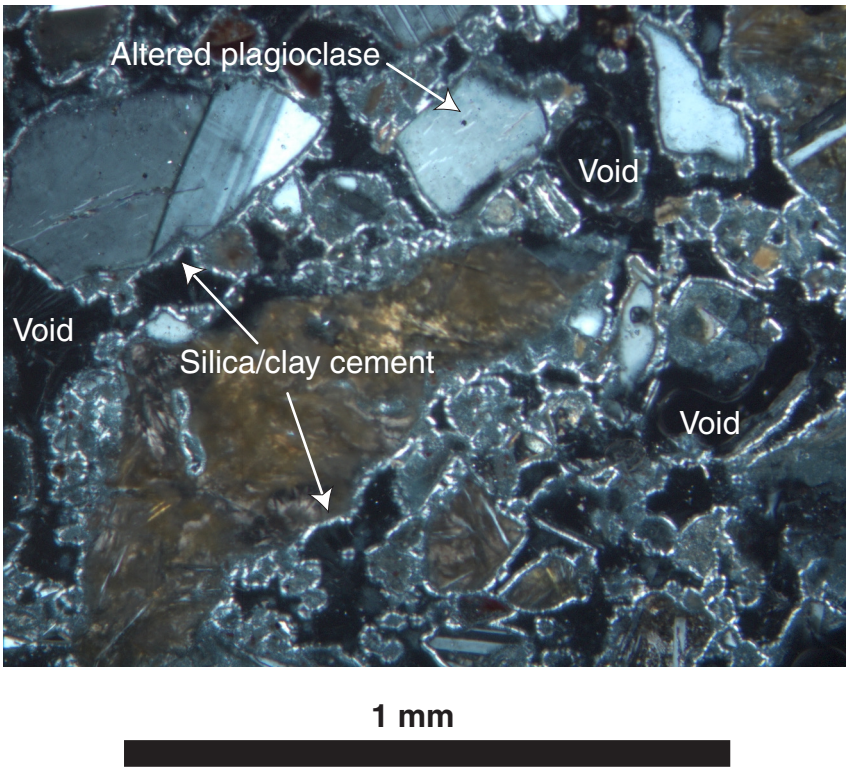

Figure F12. A. Photomicrograph, with crossed polars, of Sample 187-1161A-4R-1, 65–68 cm (see "Site 1161 Thin Sections," p. 19), showing clasts loosely cemented by cryptocrystalline silica and/or clay (birefringent material outlining clasts) in basaltic breccia matrix. **B.** Same view as A but in plane-polarized light, showing the partial filling of primary void space with Mn oxides.

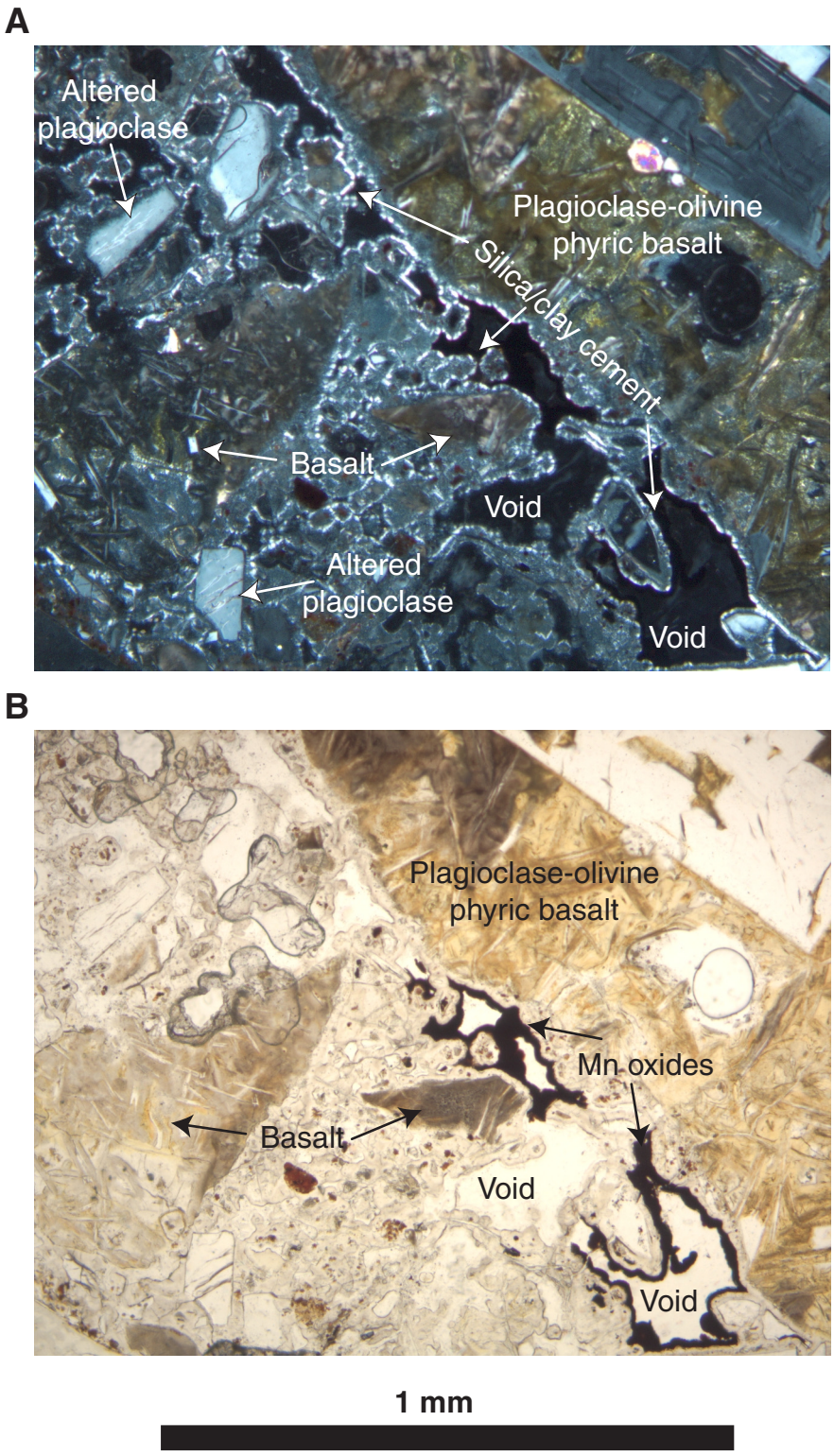

Figure F13. Photograph of interval 187-1161B-3R-1, 54–58 cm, showing microcrystalline aphyric basalt typical of Hole 1161B.

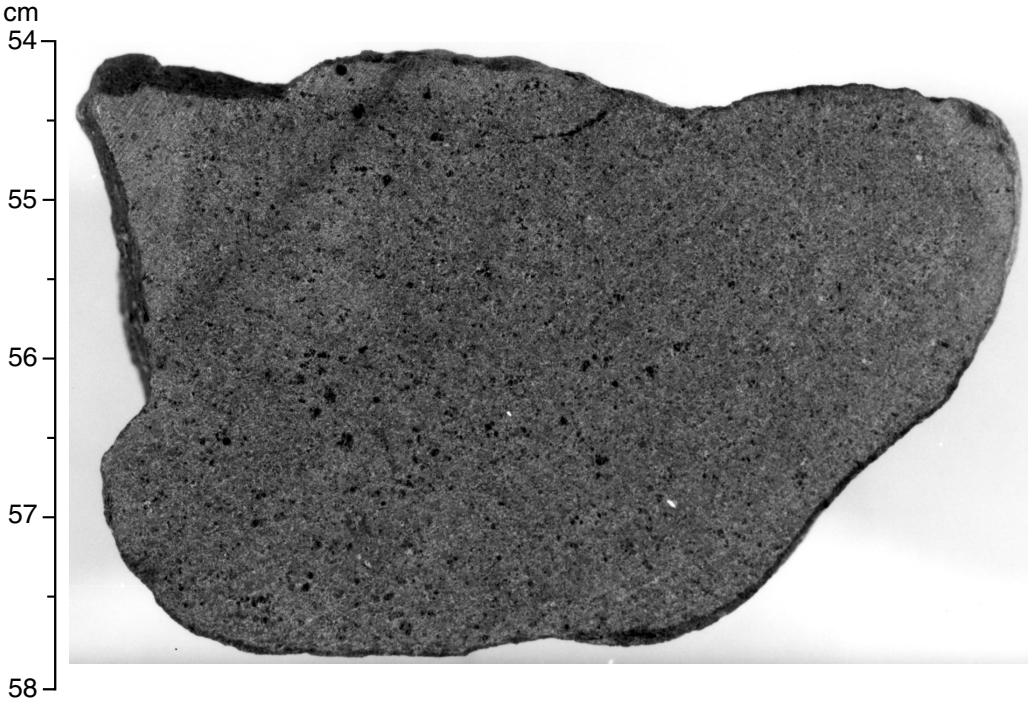

Figure F14. Photograph of interval 187-1161B-1W-1, 42–49 cm, showing plagioclase-olivine phyric basalt typical of Hole 1161B, Type 1.

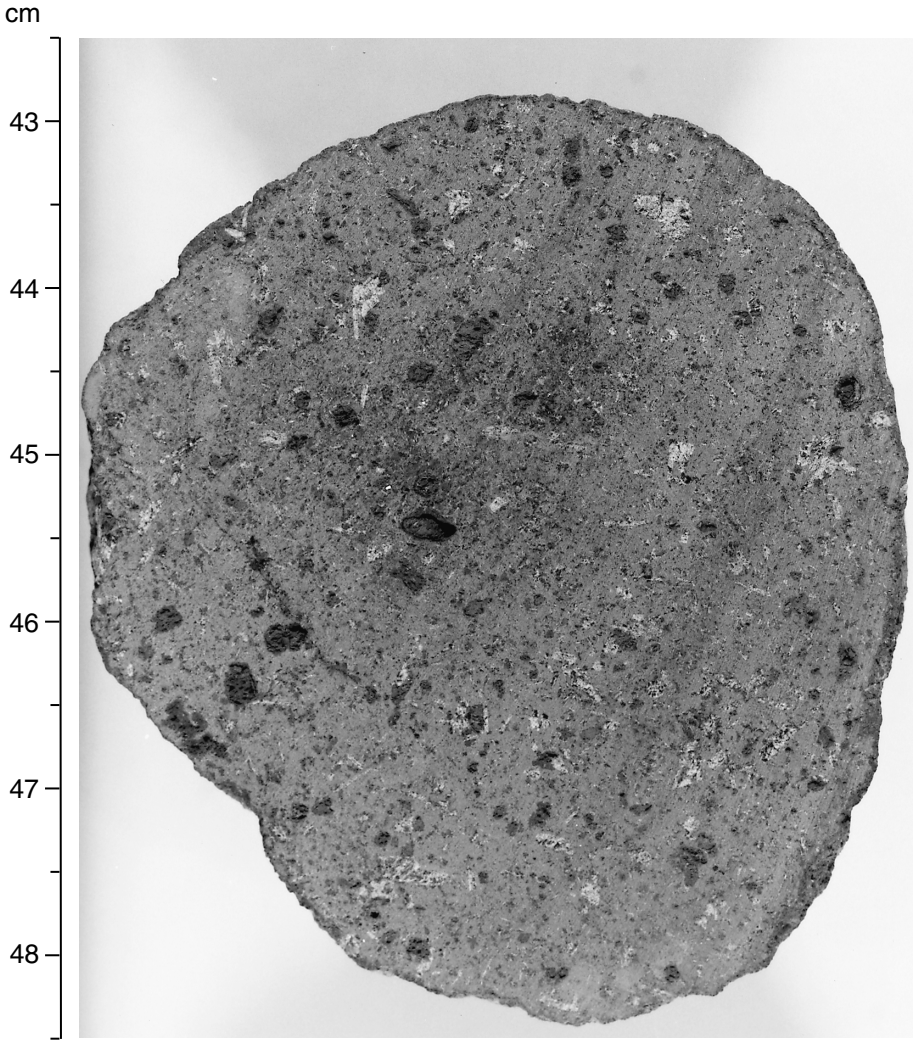

Figure F15. Photograph of interval 187-1161B-2R-1, 11–16 cm, showing a basalt breccia in which pervasively altered basaltic clasts show a range of alteration characteristics, including alteration halos and clay pseudomorphs after basalt (see "Alteration," p. 8, for a detailed discussion of these differences).

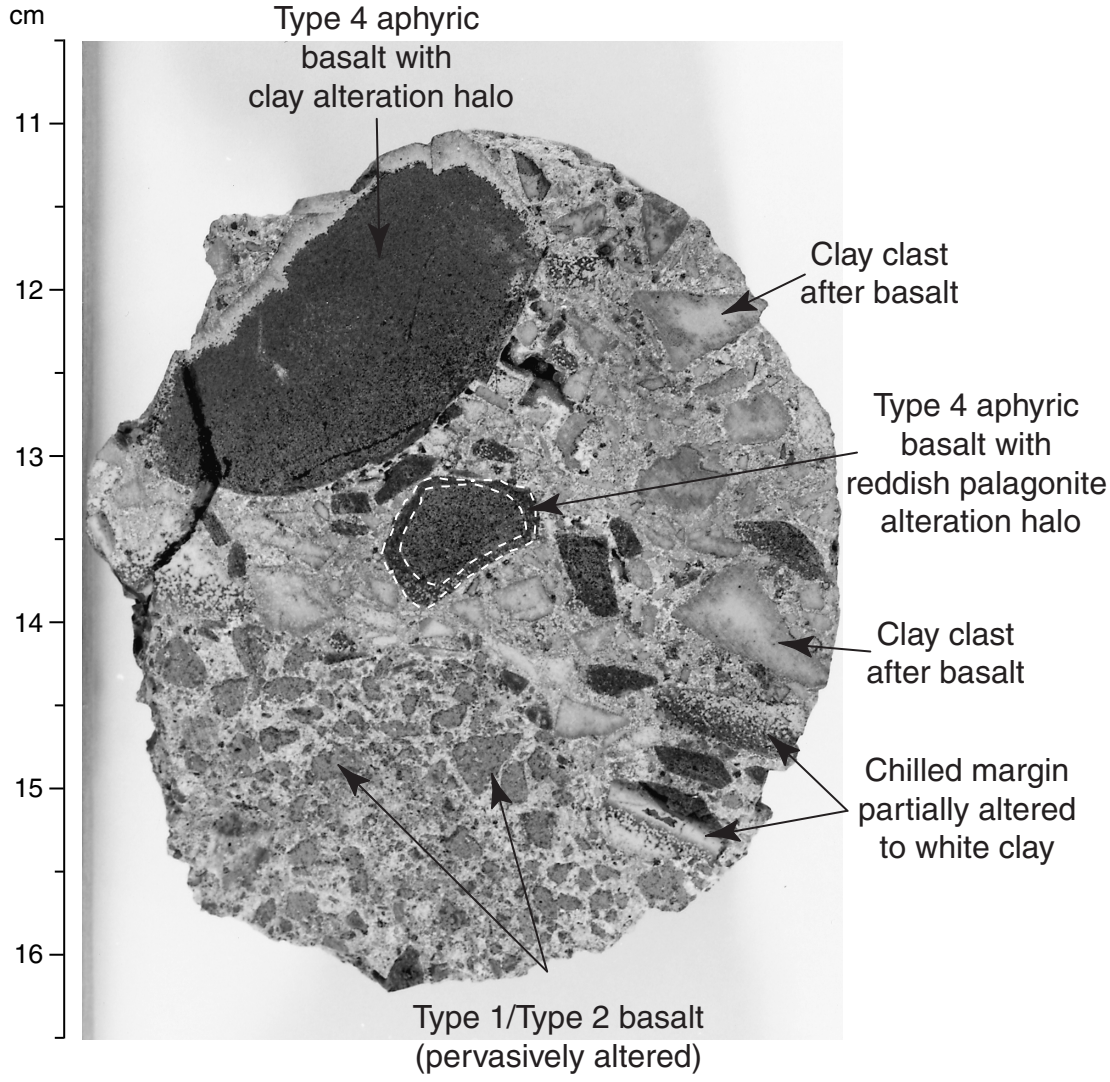

Figure F16. Photograph of interval 187-1161B-1W-1, 25–31 cm, showing basalt breccia in which the proportions of clast types vary. One part of the sample is made almost exclusively of palagonite + glass fragments, whereas the other part is dominated by microcrystalline basalt clasts. Note the chilled margin on the plagioclase-olivine phyric basalt clast between 29 and 31 cm.

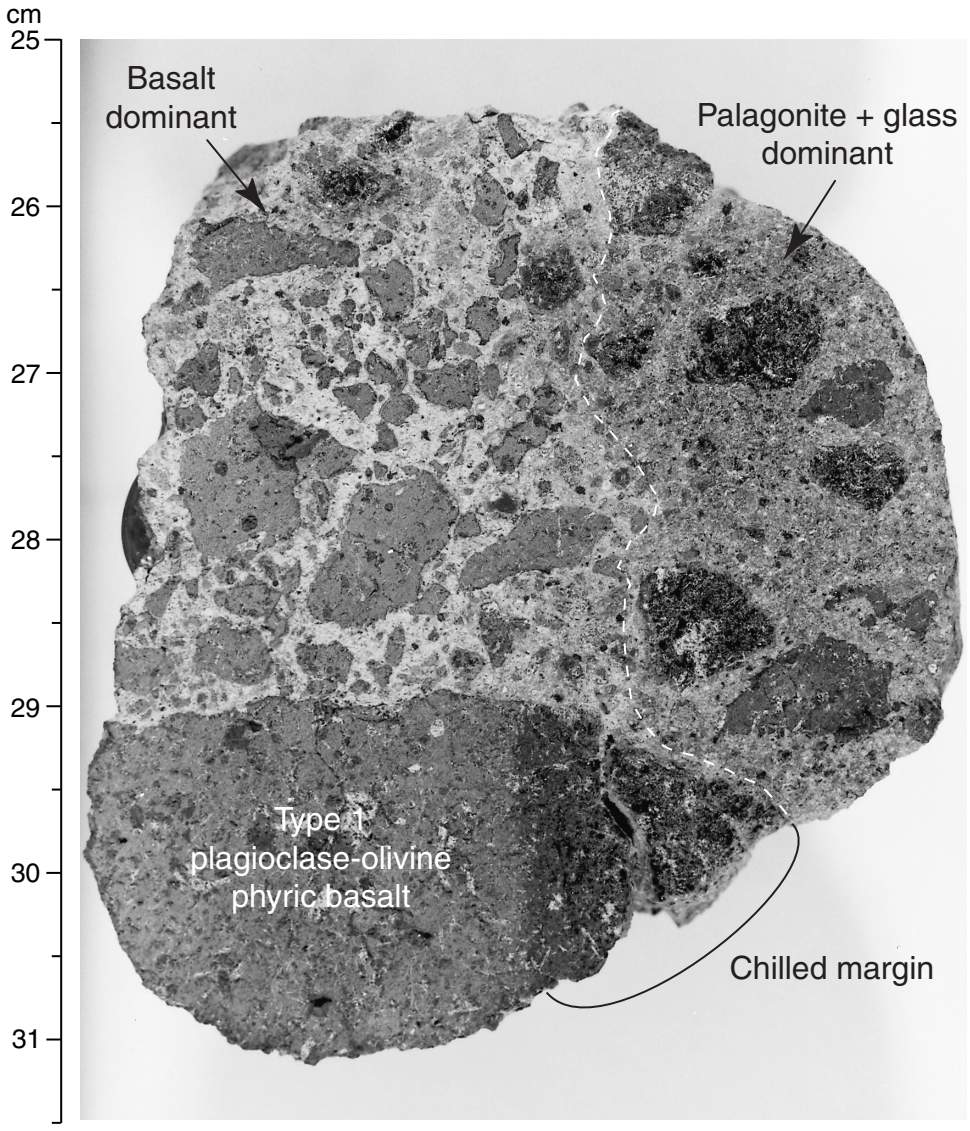

Figure F17. Photograph of interval 187-1161B-2R-1, 4–7 cm, showing a microcrystalline aphyric basalt clast with a beaded clay alteration halo and a palagonitized chilled margin in basalt breccia.

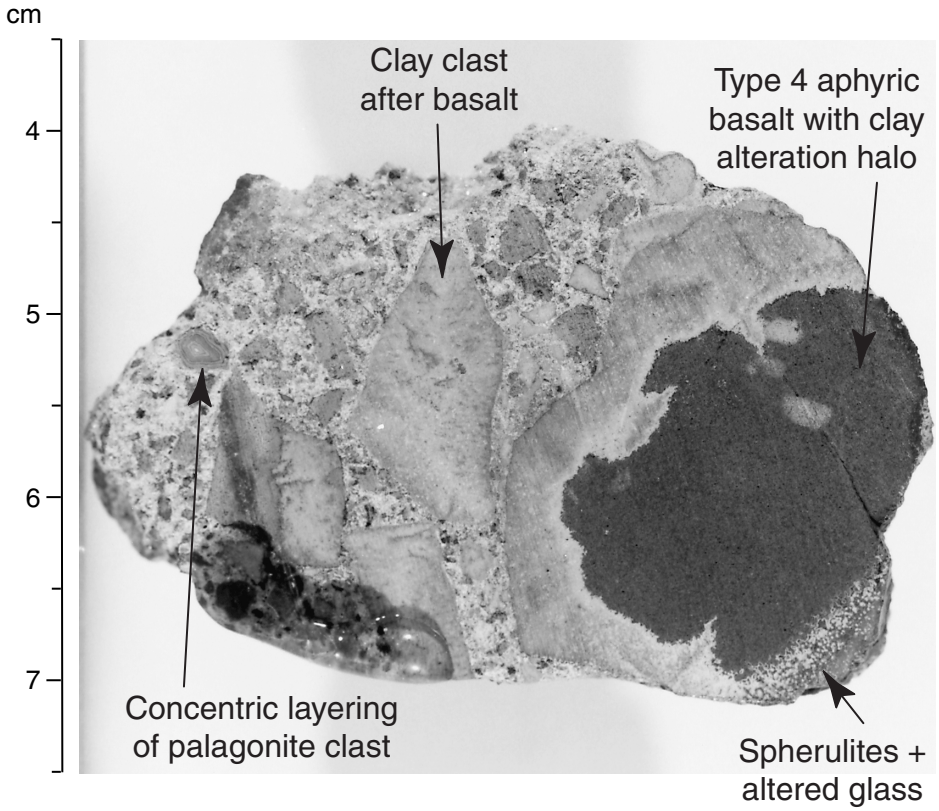

Figure F18. Photomicrograph, in plane-polarized light, of Sample 187-1161B-2R-1, 8–10 cm (see "Site 1161 Thin Sections," p. 21), showing a basalt chilled margin clast, now totally replaced by clay, in basalt breccia. Note the preservation of spherulitic texture.

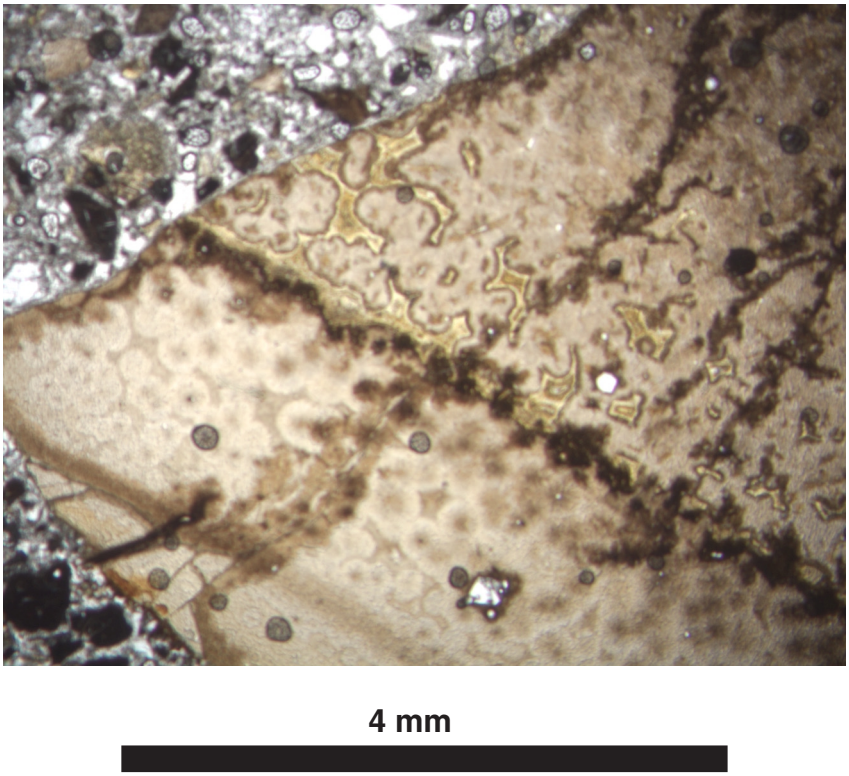

Figure F19. Photograph of interval 187-1161B-1W-1, 16–20 cm, showing palagonite + glass–rich breccia.

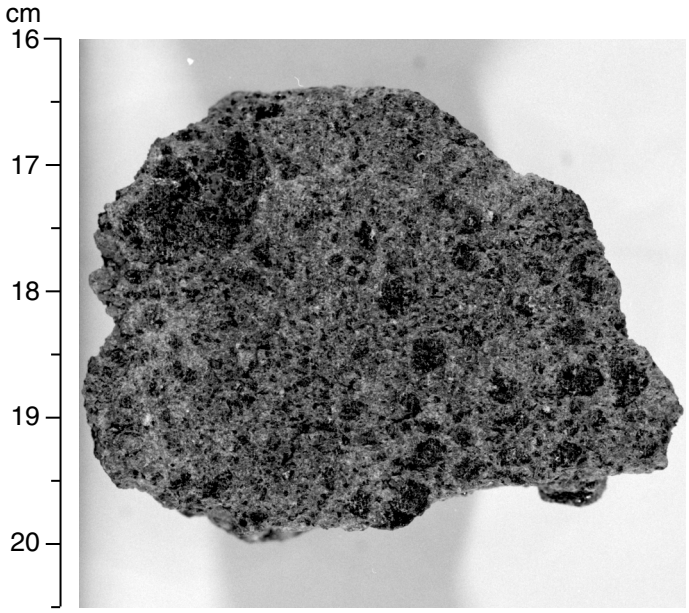

Figure F20. Photograph of interval 187-1161A-5R-1, 51–60 cm, showing basaltic breccia with a lithic matrix. Major clasts are (1) basalt and (2) basaltic glass. Both types have altered margins.

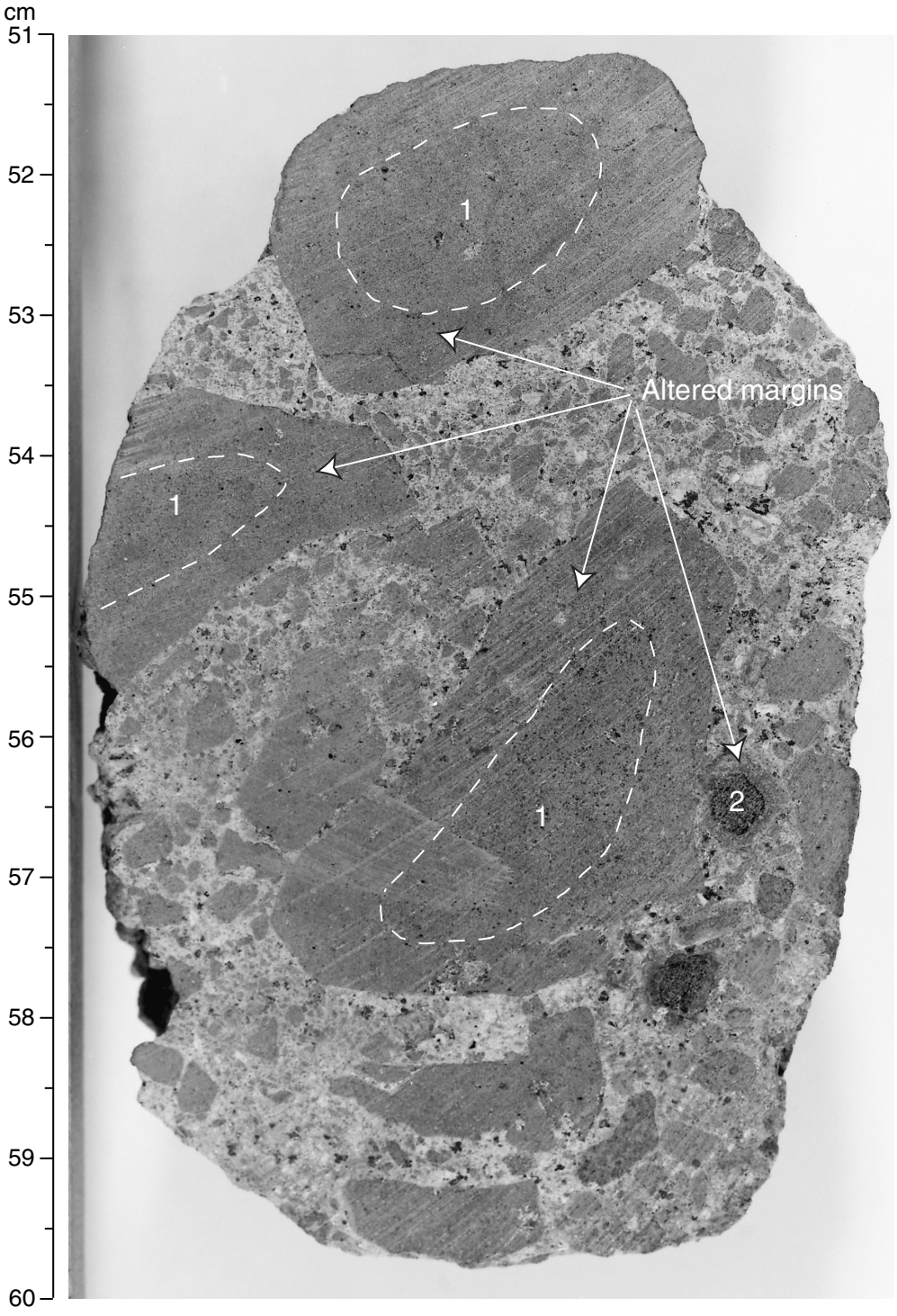

Figure F21. A. Photomicrograph, with crossed polars, of Sample 187-1161A-4R-1, 65–68 cm (see "Site 1161 Thin Sections," p. 19), showing thin silica and clay layers surrounding basaltic clasts in basaltic breccia. **B.** Photomicrograph in plane-polarized light of Sample 187-1161A-4R-1, 65–68 cm (see "Site 1161 Thin Sections," p. 19) (same field of view as A), showing Mn oxide lining voids in basaltic breccia.

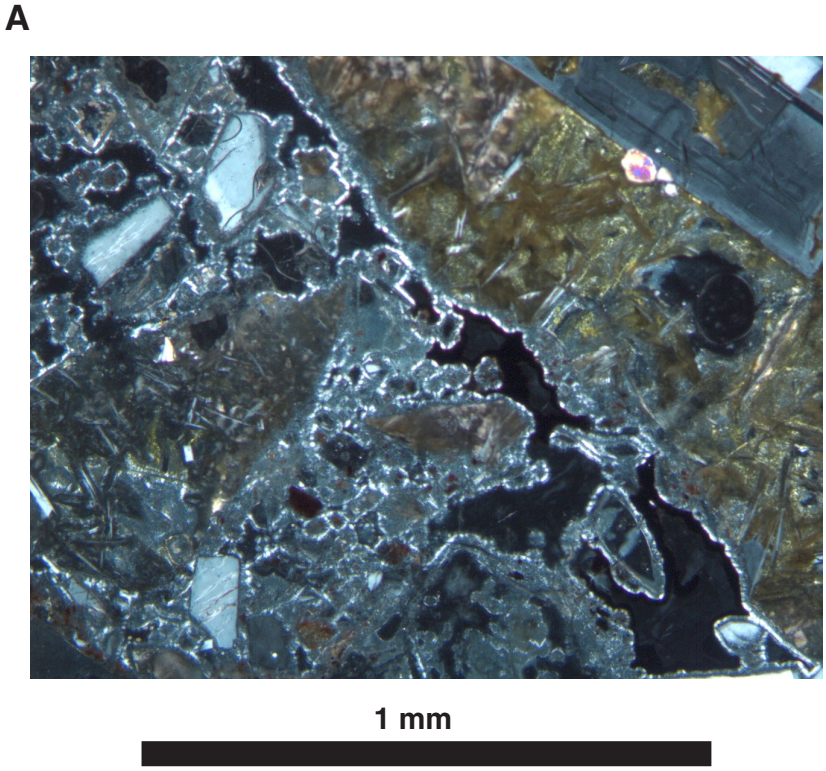

Figure F22. Photograph of interval 187-1161B-2R-1, 4–7 cm, showing a lightly altered margin of glassy basalt clast replaced by light brown gray clay in basaltic breccia. Note the spherulitic zone (lower right), which is highlighted by partial replacement by clay.

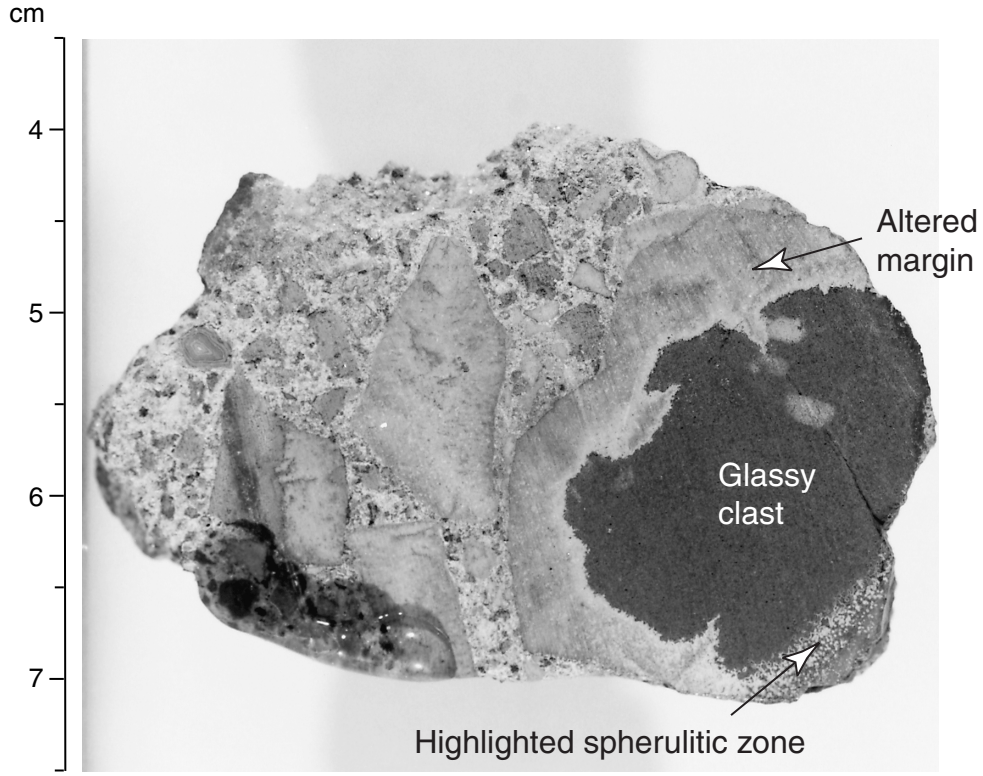

Figure F23. Photomicrograph in plane-polarized light of Sample 187-1161B-2R-1, 8–10 cm (see "Site 1161 Thin Sections," p. 21), showing radial clay aggregates replacing spherulites.

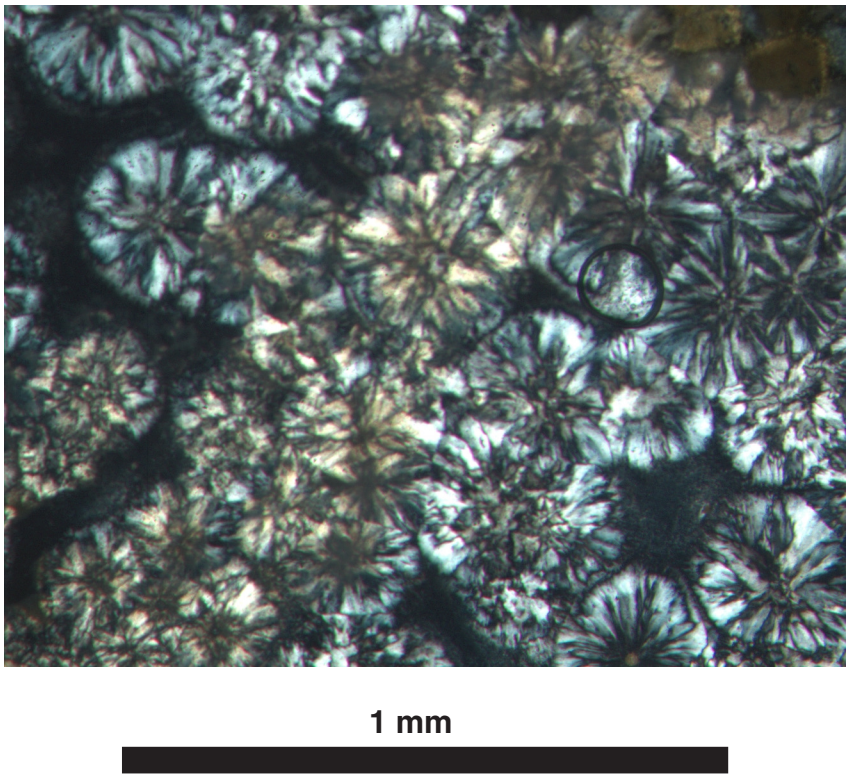

Figure F24. Photomicrograph of interval 187-1161B-2R-1, 8–10 cm (see "Site 1161 Thin Sections," p. 21), showing clast of yellow palagonite partially replaced by light brown clay.

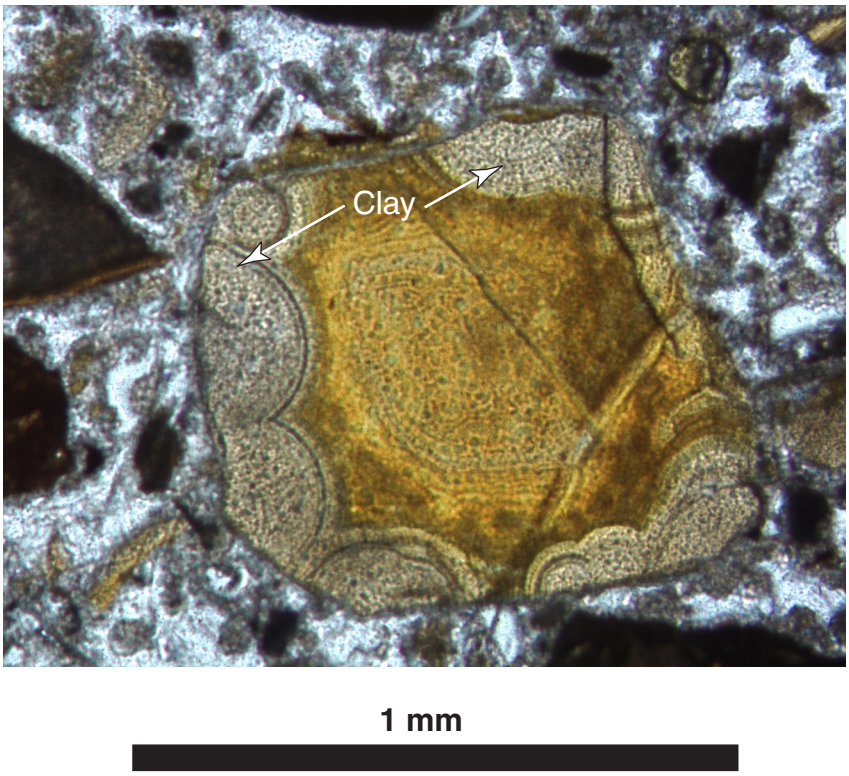

Figure F25. Photograph of interval 187-1161A-3R-1, 67–80 cm, showing fractures lined with bluish cryptocrystalline silica within the chilled margin of a pillow fragment. The inner spherulitic zone is highlighted by partial clay replacement.

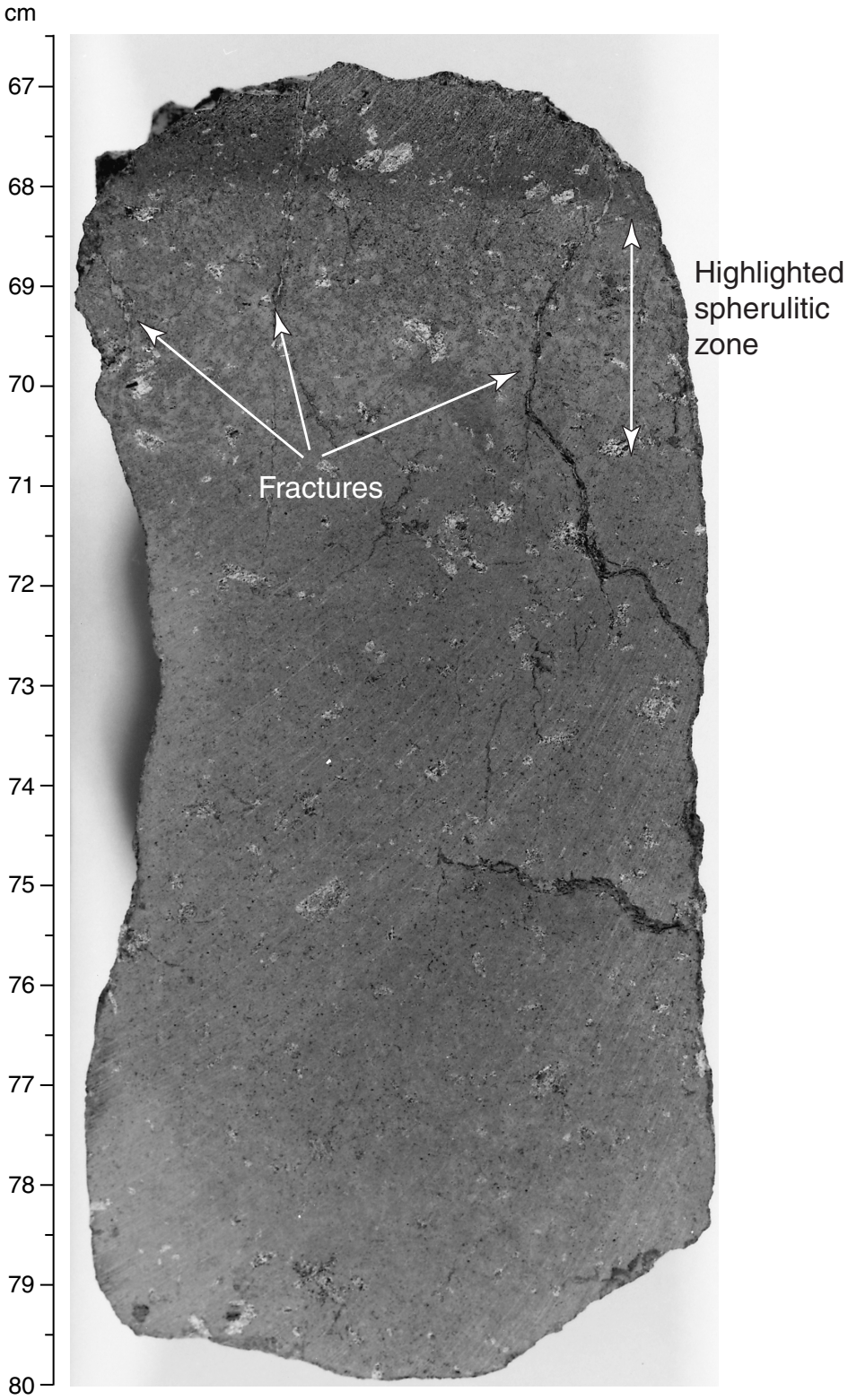

Figure F26. Photograph of Section 187-1161A-3R-1, 0.5–8 cm, showing a piece of basaltic rubble with an alteration halo around the outer edges.

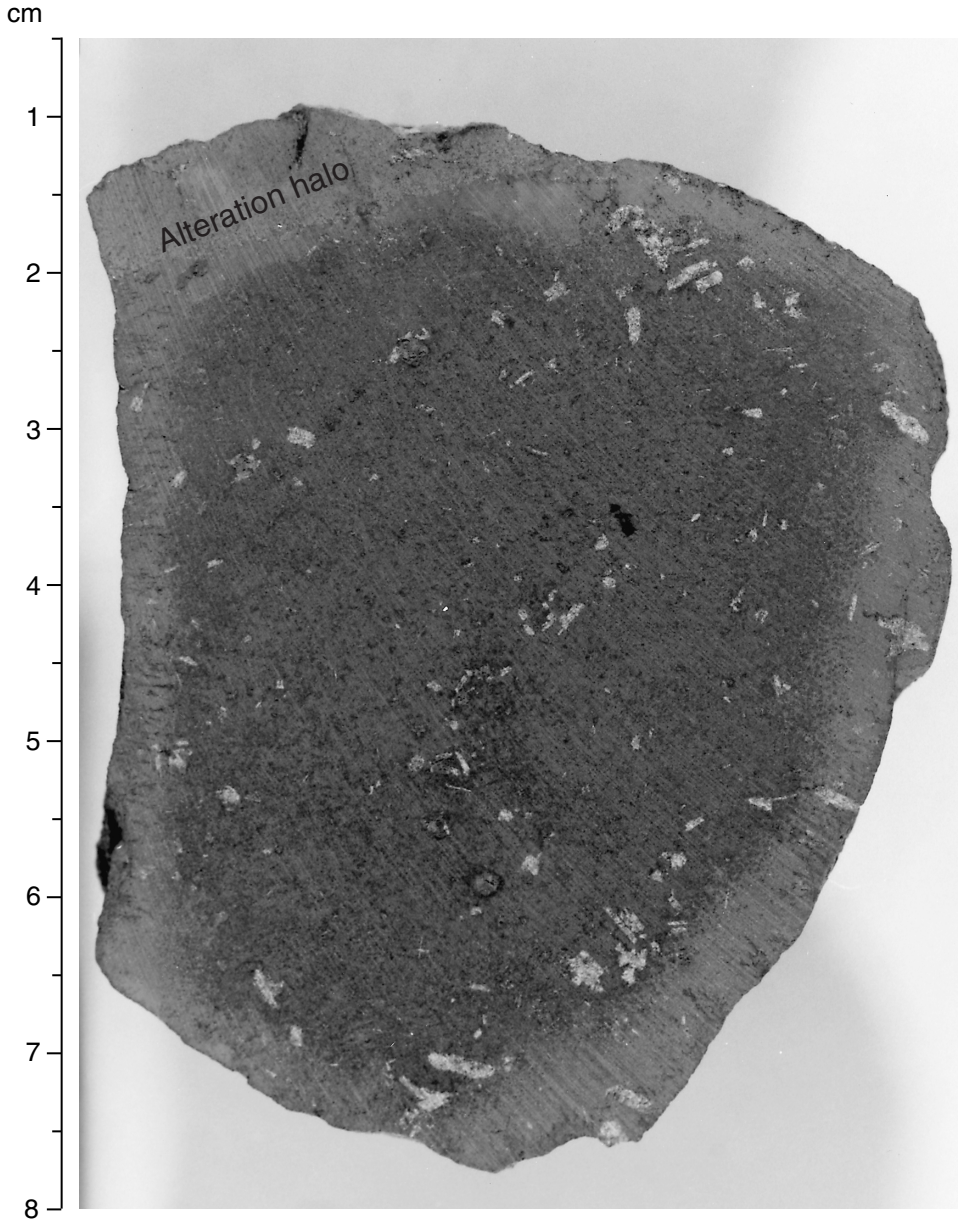

Figure F27. Photograph of Section 187-1161A-3R-1, 112–119 cm, showing replacement of basaltic glass by bluish clay and silica along fractures and cracks.

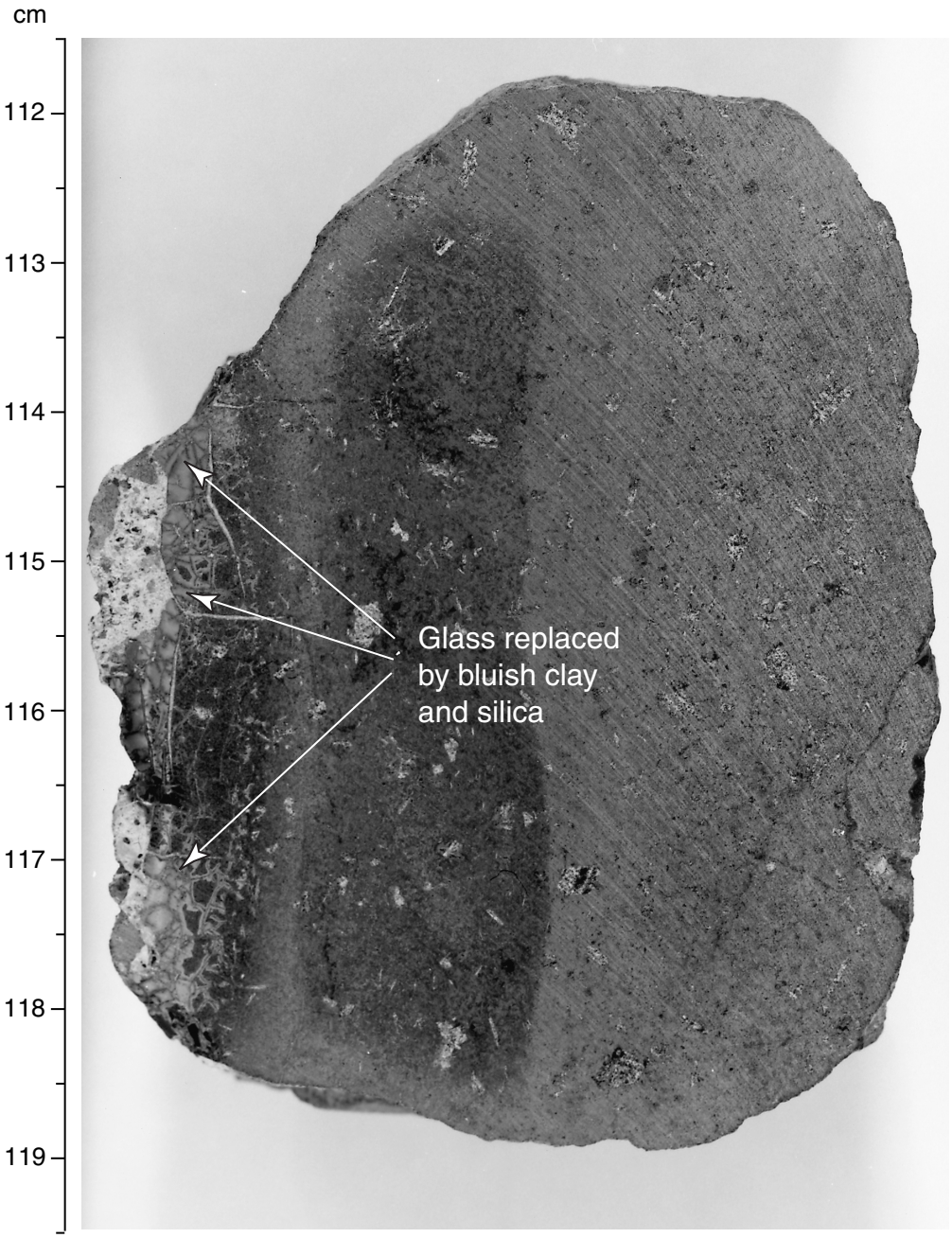

Figure F28. Photomicrograph in reflected light of Sample 187-1161A-2R-1, 10-13 cm (see **"Site 1161 Thin Sections,"** p. 16), showing composite secondary pyrite (Py), chalcopyrite (Cpy), magnetite (Mt), and hematite (Hm).

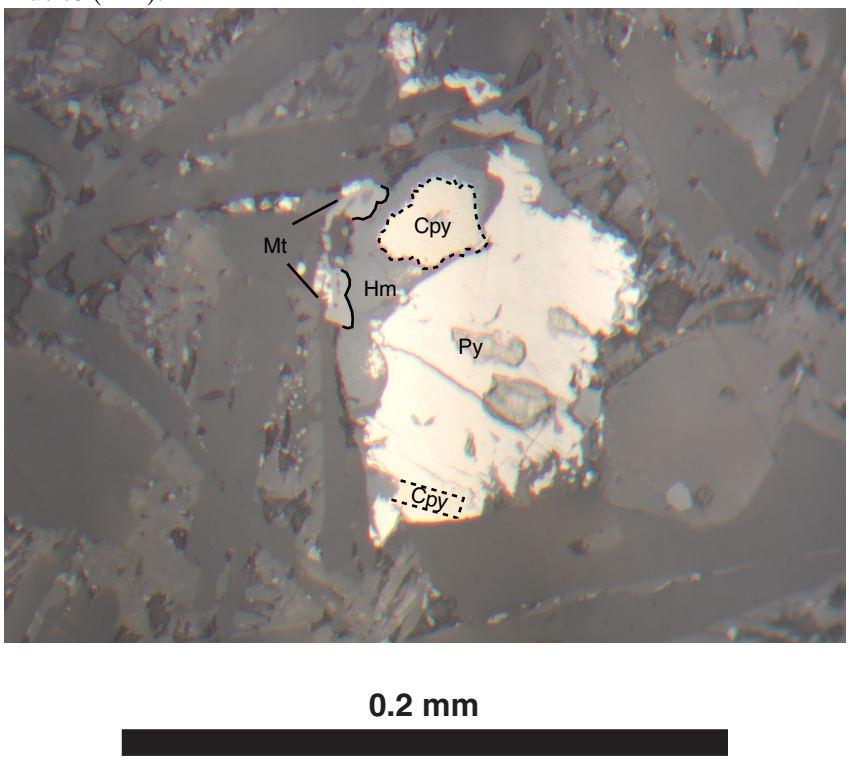

Figure F29. Major element compositions vs. MgO for Hole 1161A basalts compared with Southeast Indian Ridge glasses from Zone A. Only the averages of duplicate X-ray fluorescence or ICP-AES analyses reported in Table T4, p. 47, are plotted. PRT = propagating rift tip lavas.

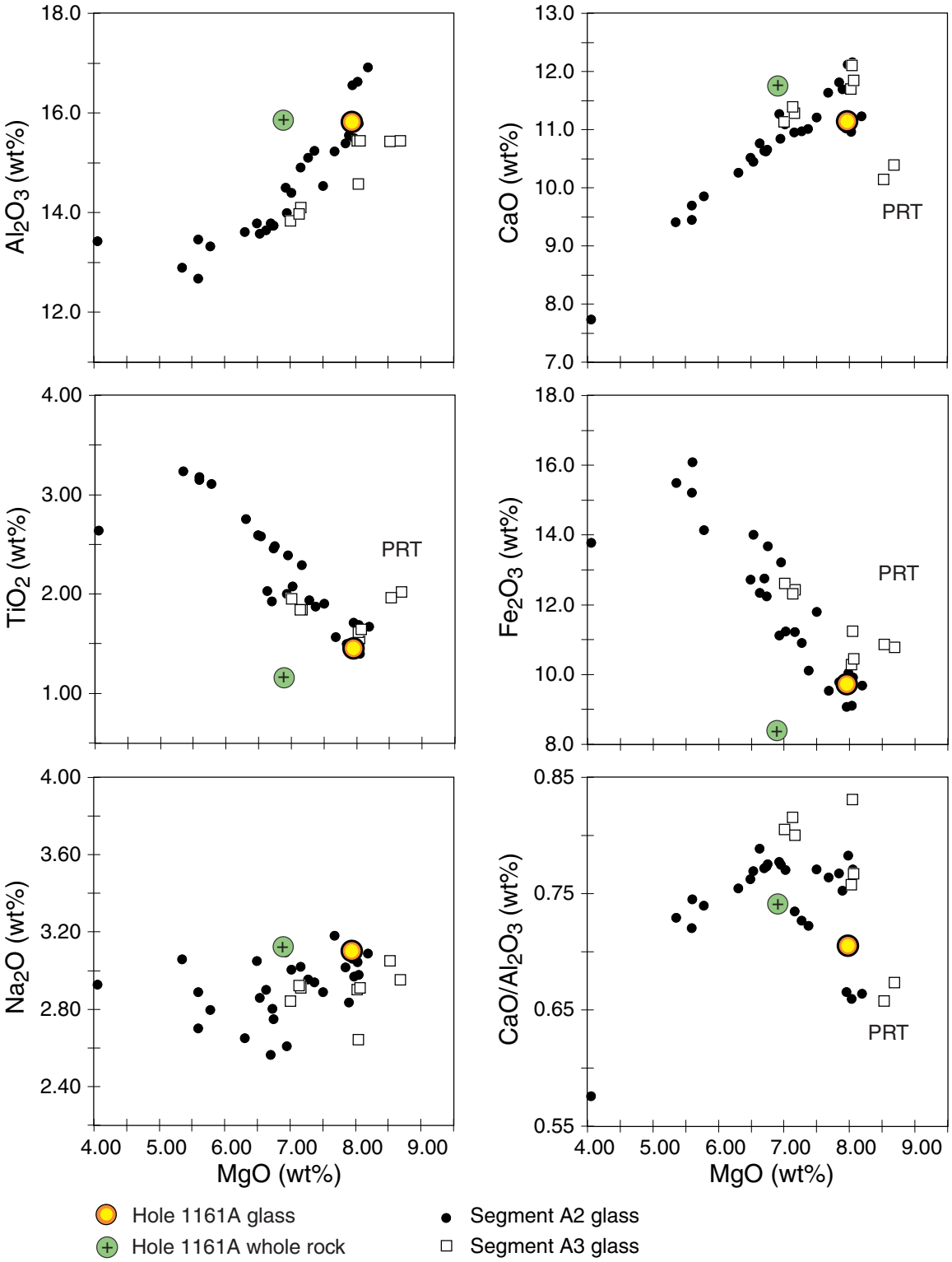

Figure F30. Trace element compositions vs. MgO for Hole 1161A basalts compared with Southeast Indian Ridge glasses from Zone A. PRT = propagating rift tip lavas.

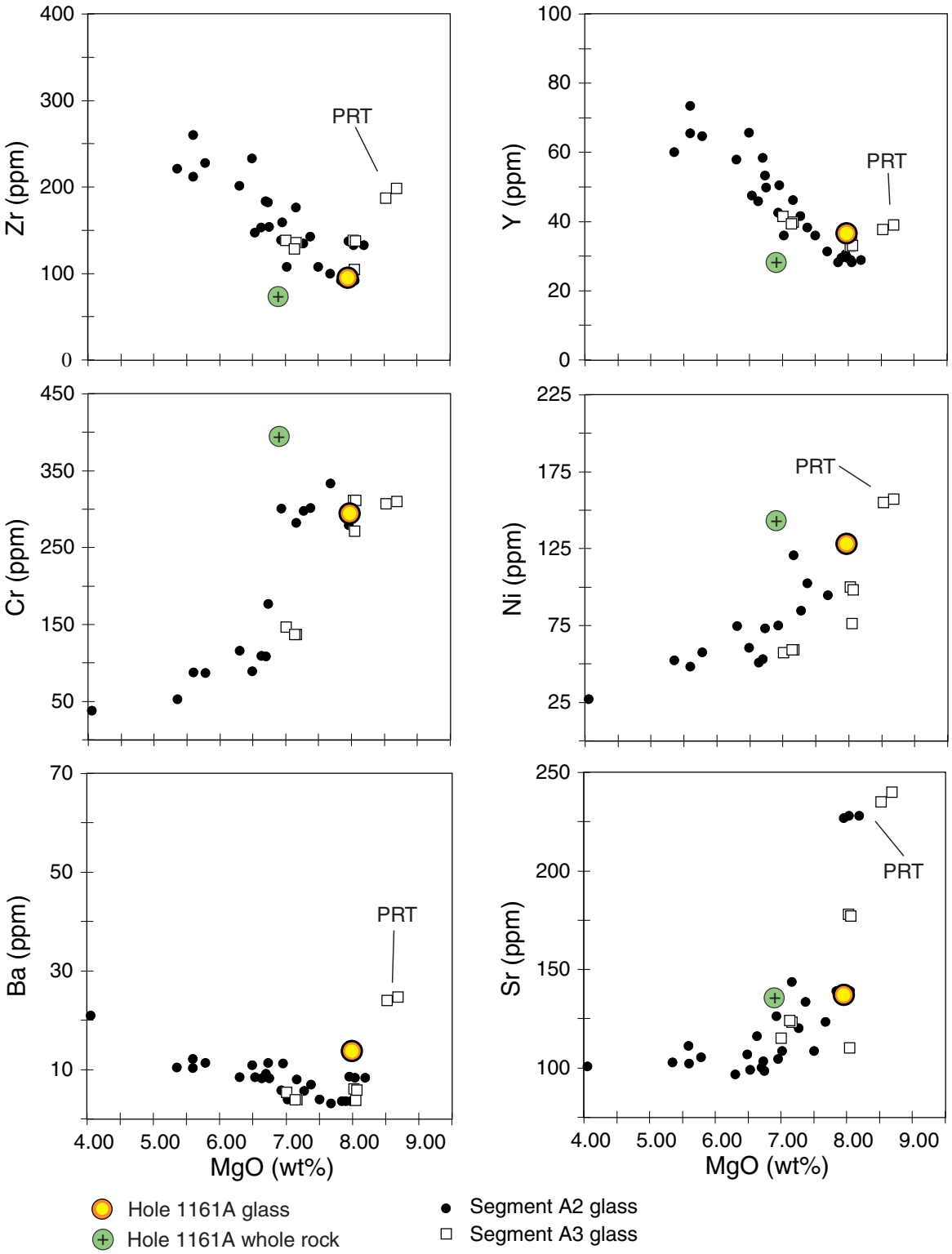

Figure F31. A. Variations of Zr/Ba vs. Ba for Hole 1161A basaltic glass and whole-rock samples compared with Indian- and Pacific-type mid-ocean-ridge basalt (MORB) fields defined by zero-age Southeast Indian Ridge (SEIR) lavas dredged between 123°E and 133°E. TP = Transitional Pacific; PRT = propagating rift tip lavas. **B.** Variations of Na_2O/TiO_2 vs. MgO for Hole 1161A basaltic glass and whole-rock samples compared with Indian- and Pacific-type MORB fields defined by zero-age SEIR lavas dredged between 123°E and 133°E. A dashed line separates Indian- and Pacific-type zero-age SEIR basalt.

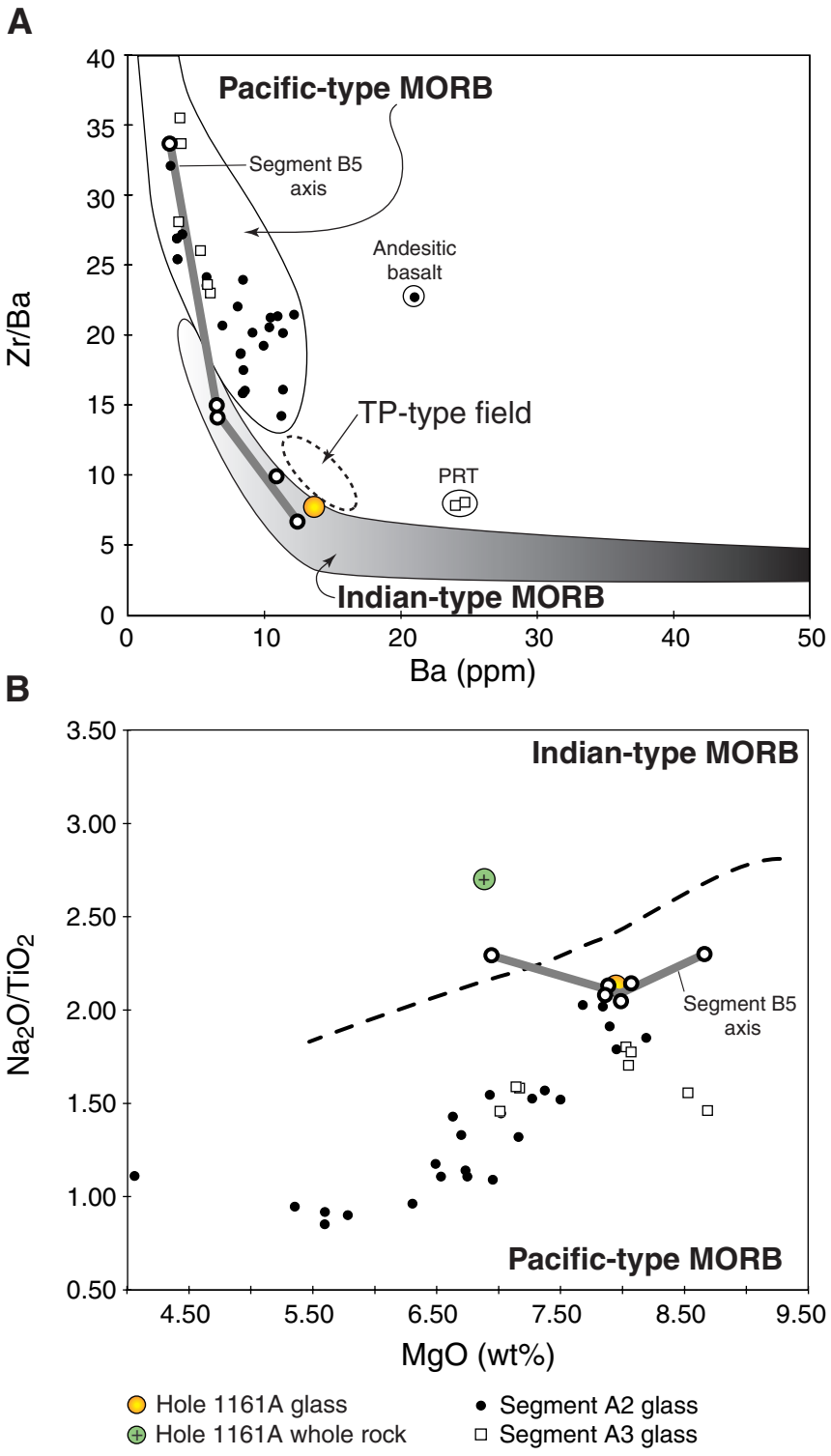

Table T1. Coring summary, Site 1161.

Hole 1161A
Latitude: 44°17.1958′S
Longitude: 129°3.0767′E
Time on hole: 1530 hr, 25 Dec 99–1315 hr, 26 Dec 99 (21.75 hr)
Time on site: 1530 hr, 25 Dec 99–0930 hr, 27 Dec 99 (42.25 hr)
Seafloor (drill-pipe measurement from rig floor, mbrf): 5031.4
Distance between rig floor and sea level (m): 11.3
Water depth (drill-pipe measurement from sea level, m): 5020.1
Total depth (from rig floor, mbrf): 176.7
Total penetration (mbsf): 145.3
Total length of cored section (m): 29.3
Total length of drilled intervals (m): 116.0
Total core recovered (m): 4.39
Core recovery (%): 15.0
Total number of cores: 4
Total number of drilled cores: 1

Hole 1161B
Latitude: 44°17.0761′S
Longitude: 129°3.0754′E
Time on hole: 1315 hr, 26 Dec 99–0930 hr, 27 Dec 99 (20.25 hr)
Seafloor (drill-pipe measurement from rig floor, mbrf): 5031.4
Distance between rig floor and sea level (m): 11.3
Water depth (drill-pipe measurement from sea level, m): 5020.1
Total depth (from rig floor, mbrf): 5198.4
Total penetration (mbsf): 167.0
Total length of cored section (m): 8.5
Total length of drilled intervals (m): 158.5
Total core recovered (m): 0.86
Core recovery (%): 10.1
Total number of cores: 2
Total number of drilled cores: 1

Core	Date (Dec 1999)	Ship local time	Depth (mbsf) Top	Depth (mbsf) Bottom	Length (m) Cored	Length (m) Recovered	Recovery (%)	Comment
187-1161A-								
1W	26	0320	0.0	116.0	116.0	1.00	N/A	
2R	26	0515	116.0	120.0	4.0	0.15	3.8	Whirl-Pak
3R	26	0720	120.0	129.4	9.4	1.75	18.6	
4R	26	0955	129.4	138.8	9.4	1.33	14.1	
5R	26	1225	138.8	145.3	6.5	1.16	17.8	
				Cored:	29.3	4.39	15.0	
				Drilled:	116.0			
				Total:	145.3			
187-1161B-								
1W	26	1925	0.0	158.5	158.5	0.53	N/A	
2R	26	2130	158.5	162.9	4.4	0.41	9.3	Whirl-Pak
3R	26	0000	162.9	167.0	4.1	0.45	11.0	
				Cored:	8.5	0.86	10.1	
				Drilled:	158.5			
				Total:	167.0			

Notes: N/A = not applicable. This table is also available in **ASCII** format.

Table T2. Summary of basalt clast types.

Type	Hole	Lithology	Color	Groundmass
1	1161A, 1161B	Sparsely to moderately plagioclase-olivine phyric basalt	Light gray	Microcrystalline
2	1161A, 1161B	Aphyric to sparsely plagioclase-olivine phyric basalt	Medium gray	Microcrystalline
3	1161A, 1161B	Aphyric basalt	Buff to gray brown	Fine grained
4	1161B	Aphyric basalt	Medium gray	Microcrystalline

Notes: Fine grained refers to groundmass composed of crystals that average ~1 mm in size. Microcrystalline groundmass requires the aid of a microscope in order to identify the crystals and, in this case, refers to a predominance of quench-crystal morphologies. This table is also available in **ASCII** format.

Table T3. Rock samples incubated for enrichment cultures and prepared for DNA analysis and electron microscope studies and microspheres evaluated for contamination studies.

Core	Depth (mbsf)	Sample type	Enrichment cultures				DNA analysis		SEM/TEM samples	
			Anaerobic	Aerobic	Microcosm*	High pressure	Wash	Fixed	Fixed	Air dried
187-1161A-										
3R	120.0-129.4	Chilled margin	8	3		X	X	X	X	X
4R	129.4-138.8	Breccia	8	3	1 Mn	X	X	X	X	X

Notes: * = microcosm for iron and sulfur or manganese (Mn) redox cycles; SEM = scanning electron microscope; TEM = transmission electron microscopy; X = samples prepared on board. This table is also available in **ASCII** format.

Table T4. Glass and whole-rock major and trace element compositions of basalts, Site 1161.

	Hole 1161A			
Core, section:	3R-1	3R-1	4R-1	4R-1
Interval (cm):	68-69	68-69	105-109	105-109
Depth (mbsf):	120.68	120.68	130.45	130.45
Piece:	12	12	20	20
Analysis:	ICP	ICP	XRF	XRF
Rock type:	Glass	Glass	Aphyric basalt	
Major element (wt%)				
SiO_2	52.23	52.70	51.03	51.56
TiO_2	1.46	1.44	1.17	1.14
Al_2O_3	15.62	15.97	15.80	15.85
Fe_2O_3	9.53	9.85	8.37	8.32
MnO	0.16	0.17	0.14	0.13
MgO	8.03	7.88	6.87	6.92
CaO	11.07	11.19	11.63	11.81
Na_2O	2.92	3.27	3.17	3.07
K_2O	0.11	0.11	0.14	0.13
P_2O_5	0.17	0.14	0.11	0.11
LOI			1.44	1.44
CO_2				
H_2O				
Total:	101.29	102.72	99.87	100.48
Trace element (ppm)				
Nb				4
Zr	103	111		83
Y	38	35		28
Sr	131	123		126
Rb				2
Zn				67
Cu				57
Ni	111	118		128
Cr	284	303		394
V				213
Ce				23
Ba	13	14		
Sc	35	38		

Notes: LOI = loss on ignition. This table is also available in **ASCII** format.